Compute Optimal Tokenization

Tomasz Limisiewicz[1], **Artidoro Pagnoni**[1], **Srini Iyer**[1], **Mike Lewis**[1], **Sachin Mehta**[1], **Alisa Liu**[2], **Margaret Li**[2], **Gargi Ghosh**[1], **Luke Zettlemoyer**[1]

[1]FAIR at Meta, [2]University of Washington

Scaling laws enable the optimal selection of data amount and language model size, yet the impact of the data unit, *the token*, on this relationship remains underexplored. In this work, we systematically investigate how the information granularity of tokens, controlled by the compression rate (i.e., average bytes of text per token), affects scaling trends. We train 988 latent tokenized models (BLT) ranging from 50M to 7B parameters that enable setting the desired compression rate. This flexibility allows us to study the role of compression rate well beyond 4.57 bytes per token obtained with a popular BPE tokenizer. Our experiments reveal that in compute-optimal configurations, model parameter counts scale proportionally to data size measured in *bytes*, not in *tokens* as commonly perceived (Kaplan et al., 2020; Hoffmann et al., 2022). Furthermore, we discover that the optimal compression rate differs from the one obtained with BPE and decreases with compute. These findings generalize to both latent and subword tokenization, as well as to languages other than English, guiding language model developers on tokenization scheme selection for maximal compute efficiency.

Date: May 4, 2026
Correspondence: tomlim@meta.com
Blogpost: https://co-tok.github.io

Meta

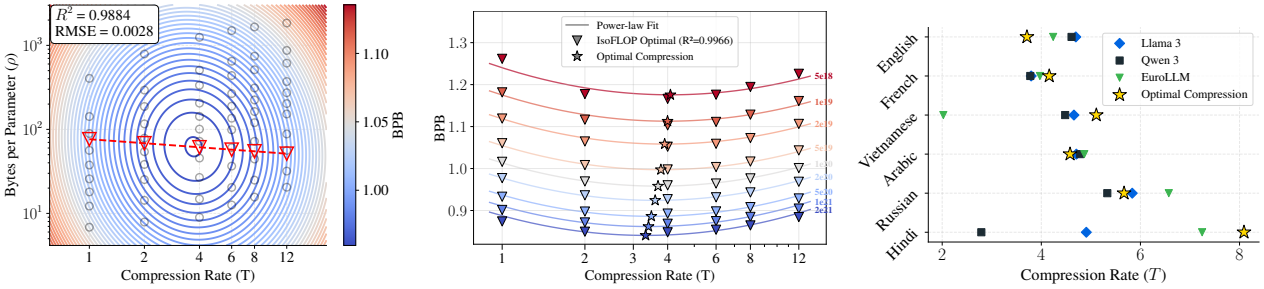

(a) Optimal bytes per parameter ratio across compression rates. Fixed training budget 10^{20} FLOPs.

(b) Optimal compression rate based on a scaling law fit. Training budget marked by color.

(c) Optimal compression rate differs from compression of subword tokenizers

Figure 1 Key findings of this work: 1a in compute optimal scaling: bytes (not tokens) of data increase proportionally to parameter count; 1b for each training budget, we find optimal compression rate, its value decreases with scale; 1c the optimal compression rate varies across languages and differs from compression of popular BPE tokenizers.

Contents

1 Introduction

Scaling laws have informed the efficient design of language models, prescribing the optimal balance between model size and training data (Kaplan et al., 2020; Hoffmann et al., 2022). Standard approaches estimate the optimal amount of data in tokens for a given compute budget (and model size). However, expressing data volume in tokens overlooks a critical aspect: the information density that each token represents. Consequently, scaling findings inherently depend on specific tokenizers and their key property: the compression rate.

To fill the research gap, we introduce laws that are aware of the compression rate T, defined as the average number of bytes per token in a given dataset. For that purpose, we need to vary the compression rate without changing the vocabulary size (and thus the number of parameters). Therefore, in our experiments we rely on Byte Latent Transformer (BLT, Pagnoni et al., 2025), a recent architecture that segments byte-level input in a latent space. BLT's latent tokenization is a robust tool for this purpose, as it allows us to precisely adjust the compression rate by setting an average segment size.[1] Additionally, compression plays a significant role in subword tokenization. We can order popular subword methods by their compression rate: from pure byte or character-level segmentation ($T \approx 1$) (Xue et al., 2022; Wang et al., 2024), through widely used BPE ($T \approx 4.57$) (Sennrich et al., 2016), to SuperBPE ($T \approx 6.16$) (Liu et al., 2025), which achieves high compression by allowing multi-word tokens.[2]

In the context of scaling, compression rate impacts model efficiency in both training and inference. Increasing compression allows the same data to be represented with fewer tokens, directly reducing the computational cost of processing. The unlocked savings in FLOPs (unit of computation) can be used to increase training data, model size, or both, without increasing the total computation budget.

To the best of our knowledge, this is the first thorough study of the effect of compression rate on the compute efficiency of language models. We pose the following research questions:

[R1]*: How does compression rate impact the compute-optimal ratio between parameters and data?* This question concerns the unit of data we should use in model scaling. We investigate whether the compute-optimal ratio is best expressed in tokens or bytes (which are the underlying unit of text encoding). For example, given the Chinchilla rule of thumb of training on ≈ 20 tokens per parameter (Hoffmann et al., 2022), does this ratio hold as we increase compression, or should the ratio of bytes to parameters remain constant given a dataset of English texts?

[R2]*: Is there an optimal compression rate for specific datasets?* We investigate whether there exists a compression rate that yields the lowest loss for a fixed compute budget, assuming the optimal data to parameter ratio. Furthermore, we examine whether this optimal compression rate shifts with the compute budget or dataset domain.

[R3]*: Is the impact of compression rate on scaling trends similar for latent and subword tokenized models?* Does the answer to the previous questions depend on the tokenization method? We conduct experiments on subword-tokenized models to validate if the scaling trends match those observed for BLT.

[R4]*: Is optimal compression rate language specific?* We extend our experiments to languages other than English to test whether optimal data to parameter ratio and compression rate change depending on language. We hypothesize that both will grow proportionally to *parity*, defined as the ratio of byte length of parallel sentences expressed in two languages (Petrov et al., 2023; Ahia et al., 2023).

The structure of the paper is as follows. In Section 2, we describe our experimental setting, including details of the datasets, models, and methods for deriving power laws. In Section 3, we present experiments scaling BLT across a wide range of compression rates to answer **[R1]** and **[R2]**. In Section 4, we examine subword-tokenized

[1] Recent latent tokenized models allow achieving a wide range of compression rate, similarly to BLT. However, in other approaches compression rate cannot be precisely controlled due to reliance on a segment boundary predictor (Hwang et al., 2025; Nawrot et al., 2023) or whitespace supervision (Neitemeier et al., 2025; Slagle, 2024; Videau et al., 2025).

[2] Estimates of compression rate are computed for DCLM corpus (Li et al., 2024) consisting of "plain English" texts.

models to compare with the findings from the previous section and address **[R3]**. Finally, in Section 5, we extend our scaling experiments to languages other than English to answer **[R4]**.

2 Methodology

In this section, we provide details on the language models used and experimental setup. We also describe the evaluation and the procedure for fitting power laws to estimate the optimal data-to-parameter ratio and loss.

2.1 Model Architectures

For all experiments, we train Transformer models (Vaswani et al., 2017) of varying parameter sizes, adhering to Llama 3 architectural choices (Llama Team, AI @ Meta, 2024). We follow a standard scaling recipe: increasing models' width and depth in a 1:1 ratio, meaning the number of heads equals the number of layers. The latent dimension size is set to 128 times the number of heads, and the feed-forward network uses 4× upscaling.

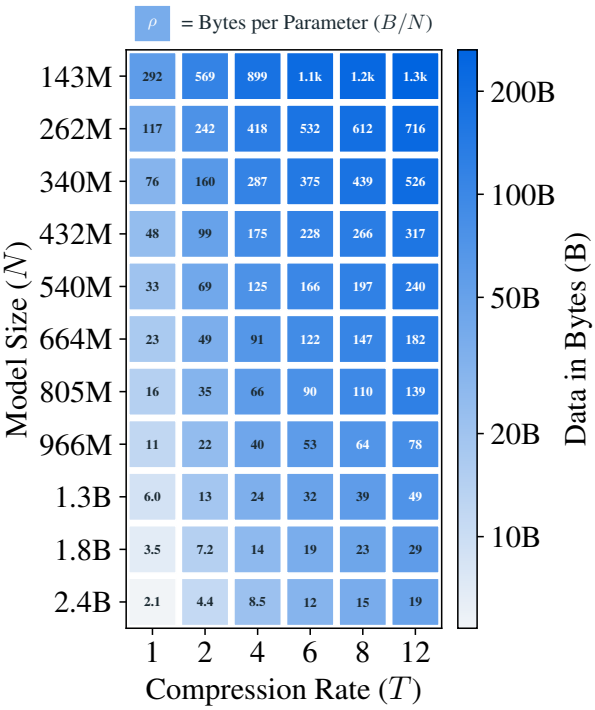

Figure 2 The grid of experiments for the budget of $C = 10^{20}$ FLOPs. For each compression rate T (x-axis) and model size N (y-axis) we can read amount of training data B (color) and the corresponding bytes per parameter ratio ρ (values in squares).

Latent Tokenized Models These models feature a hierarchical architecture comprising three modules: (1) an encoder that aggregates byte-level representations into latent tokens; (2) a global module operating on these latent tokens (the Transformer model described above); and (3) a decoder that maps latent representations back to the byte level for next-byte prediction. We adopt the Byte Latent Transformer (BLT) architecture (Pagnoni et al., 2025). BLT utilizes entropy spikes to segment byte sequences into latent tokens, allowing us to control the compression rate by adjusting the entropy threshold. Cross-attention mechanisms implement the mapping between latent and byte embeddings. A key deviation from the original BLT implementation is the omission of hash embeddings for byte n-grams. We omit these because n-grams can span more bytes than the latent tokens themselves, potentially interfering with the target compression rate. We also introduce a modified scaling recipe for the local modules (encoder and decoder), observing that prioritizing width over depth gives better performance. The exact scaling recipe is presented in Appendix A.

Subword Tokenized Models We employ standard isotropic models following the Llama 3 architecture (Llama Team, AI @ Meta, 2024).[3] By analogy to hierarchical models, subword embedding and de-embedding layers correspond to local modules. Unlike latent models, the compression rate (T) of subword models is not directly controllable but is determined by the tokenization method, tokenizer's training corpus and vocabulary size (V). To obtain a wide range of compression rates, we train language models using different subword tokenization algorithms. Specifically: character tokenization ($T = 1.01$, $V = 148,000$) the BPE tokenizer of Llama 3 ($T = 4.57$, $V = 126,000$); and the SuperBPE tokenizer, which allows merging multiple words into one token (Liu et al., 2025) ($T = 6.16$, $V = 200,000$).[4] We also analyze versions of the Llama 3 tokenizer

[3] In this context, *isotropic* means that all modules of the model operate on sequences of the same granularity, unlike in hierarchical models.

[4] For low compression we choose character level tokenization instead of byte level to match the magnitude of vocabulary size across isotropic models. In Appendix F.5, we show that character and byte models achieve similar performance at large scale.

with 75% and 90% of vocabulary masked, obtaining compression rates of $T = 4.16$ and $T = 3.71$ respectively. Even though the vocabulary is masked in these models, we still consider the original $V = 126,000$ for FLOPs computation. The compression rates T are estimated on the DCLM dataset used in training.

The exact specifications for all models used in our study are presented in Appendix A.

2.2 Training and Evaluation

We train models under compute budgets (C) expressed in FLOPs, ranging from 5×10^{18} to 2×10^{21} FLOPs. If not stated otherwise, we use exact computation of training FLOPs, instead of an approximation. In total, we train 988 latently and 320 subword tokenized models with sizes from 50M to 6.7B parameters on training data of sizes from 4B to 1.1T bytes.

For each budget C, we vary the parameter size (N) and compression rate (T). The parameters N and compression rate T uniquely determine the training data amount in bytes (B). Consequently, for each compute budget, we obtain a grid of models corresponding to the cartesian product of T and N. For each of the configurations, we compute the bytes per parameter ratio (ρ), as shown in Figure 2. For BLT, we test six compression rate values $T \in \{1, 2, 4, 6, 8, 12\}$, while for subword models, compression rate is determined by the tokenizer $T \in \{1.01, 3.71, 4.16, 4.57, 6.16\}$. For all training runs, we fix the batch size at 2 million bytes and the learning rate at 4×10^{-4}. We use the AdamW optimizer (Loshchilov and Hutter, 2019) with a warmup-stable-decay learning rate schedule.

Unless stated otherwise, we train on DCLM (Li et al., 2024), a dataset of plain English texts selected to limit data mixing across domains and languages. Data mixing could cause non-uniform granularity of information and thus confound our analysis. We evaluate models on the C4 validation split (Raffel et al., 2020).

To compare loss across different models with various tokenization methods, we evaluate models using bits-per-byte (BPB), which is loss divided by the number of bytes in the evaluation texts. In each training and evaluation example, we fix context to contain the same number of 8192 bytes (e.g., with compression rate $T = 4$ we evaluate on 2048 tokens per example, then with compression rate $T = 8$ we evaluate on 1024 tokens).

2.3 Fitting Power Laws

We fit the parameters for power laws presented in the next section using the BFGS optimizer (Liu and Nocedal, 1989; Zhu et al., 1997) minimizing sum of squares loss. To ensure reliability, we initiate optimization from multiple random seeds and compute confidence intervals using a numerical approximation of the Hessian. Further details on the fitting procedure can be found in Appendix B.

3 Scaling Laws and Data Compression

In this section, we present scaling results for BLT models revealing the role of data compression rate. We fit scaling laws in two stages, as such an approach shows more faithful approximations (Li et al., 2025). In the first stage, we estimate the optimal training data size in bytes $B^\star$ and model size $N^\star$ as a power law function of compute budget C and compression rate T, addressing research question **R1**. Subsequently, in the second stage, we model the dynamics of the optimal loss $L^\star$ obtained for the found $B^\star$ and $N^\star$ configuration. We examine the effect of compression rate T on $L^\star$ to answer research question **R2**.

3.1 Scaling Law I: Optimal Data and Parameters

For each compute budget C and compression rate T, we identify the optimal training data size by fitting a second-degree polynomial (i.e. IsoFLOP) to the relationship between log-data $\log(B)$ and validation loss L. The optimal data size $B^\star$ corresponds to the minimum of this parabola. We determine the corresponding optimal parameter count $N^\star$ via log-linear interpolation.

In the first power law we estimate the optimal training data size $B^\star$ as a power law function of compute budget C and compression rate T:

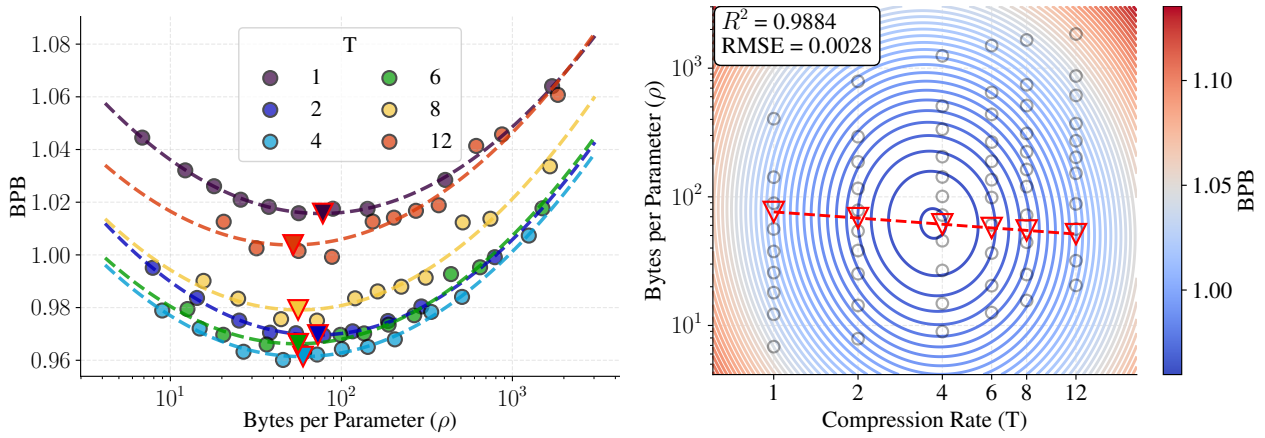

(a) 2D IsoFLOP **(b)** 3D IsoFLOP (heatmap)

Figure 3 Evaluation scores of latent tokenized models on C4 test set with fixed FLOPs budget ($C = 10^{20}$), compared against bytes per parameter ratio. 2-dimensional IsoFLOP (parabola) were fitted for each compression rate, while 3-dimensional IsoFLOP jointly for all compression rates (on x-axis). Minima of both fits show that minimal loss is obtained at almost constant value of bytes per parameter ratio $\rho \approx 60$. For IsoFLOPs as function of data, parameters, and for other compute budgets, refer to Appendix F.1

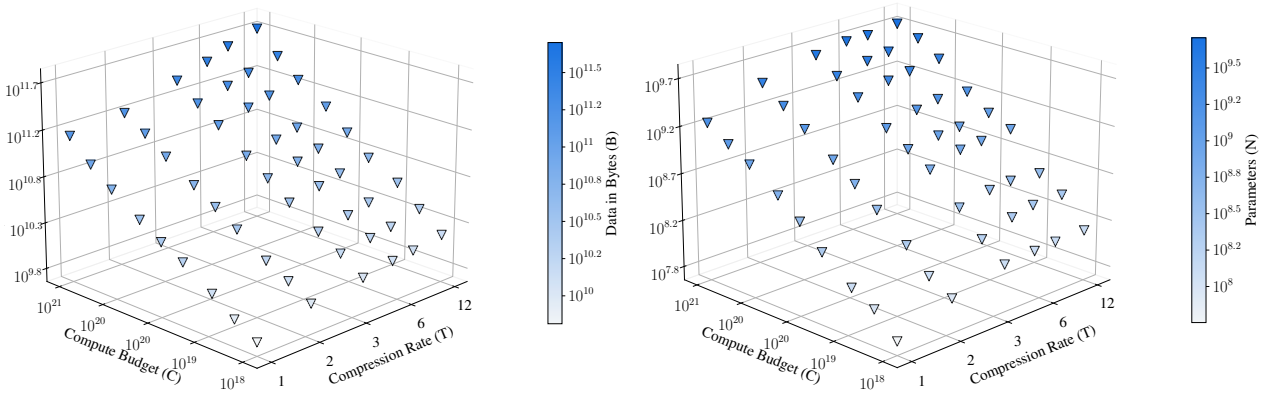

(a) Amount of data **(b)** Model size

Figure 4 Optimal data and model size configurations for each compute budget and compression rate (latent tokenized models).

$$B^\star(C,T) \cong B_0 C^\alpha T^\beta \tag{1}$$

This equation involves three parameters: B_0 (initial optimal data), α (scaling with compute), and β (scaling with compression). In this fit, for simplicity and better generalization across tokenizers, we consider only the parameters of the latent module (i.e., excluding encoder/decoder parameters for BLT and embedding parameters for subword models). Importantly, given our fixed scaling recipe, the number of the model's "latent" parameters determines the "total" parameter count. We can approximate the latent module's compute C as:

$$C \approx 6N\frac{B}{T} \tag{2}$$

Where $\frac{B}{T}$ is the amount of data expressed in tokens, typically denoted as D in other scaling laws works. Solving Approximation 1 allows us to obtain a power trend for optimal global parameter count:

$$N^\star(C,T) \cong \frac{1}{6B_0} C^{1-\alpha} T^{1-\beta} = N_0 C^{1-\alpha} T^{1-\beta} \tag{3}$$

We also define the optimal Byte-per-Parameter ratio, $\rho^\star = B^\star/N^\star$. Based on the derived power laws, this ratio has the following form:

$$\rho^\star(C,T) \cong \frac{B_0}{N_0} C^{2\alpha-1} T^{2\beta-1} \tag{4}$$

Before observing the actual fit, we can describe the meaning of specific hypothetical values of α and β.

- When $\alpha \approx 0.5$, $\rho^\star$ would remain constant for varying values of compute budget C. This would mean that data and parameters should be scaled in 1:1 proportion. Similar equivalence was observed in Hoffmann et al. (2022).
- Analogously $\beta \approx 0.5$, would indicate that compute unlocked with higher compression should be allocated equally in increase of parameters and training data. Hence, the optimal bytes per parameter $\rho^\star$ would remain constant across varying compression rates T.
- $\beta \approx 1$ would indicate that we can omit the notion of compression from scaling laws and replace B (amount of data in bytes) with used $D = \frac{B}{T}$ (amount of data in tokens). Such observation would suggest that we should simplify the scaling law to consider data amount in tokens $D^\star$ and neglect the impact of compression (as done in previous scaling studies).

3.2 Scaling Law I: Results

The IsoFLOPs analysis shows that for a set compute budget C, a second degree fit faithfully describes the relationship between logarithm of data size $\log(B)$ and validation loss L (see Figure 19 in Appendix). Therefore, we can easily identify the optimal data size $B^\star$ by finding the minimum of the parabola (or paraboloid in the three-dimensional case).

Moreover, the results empirically confirm that the optimal data and parameter count gradually increase with increasing compression rate T, thanks to a decrease in compute cost per byte. Figure 3 indicates that across compression rates the optimal byte-per-parameter ratio $\rho^\star$ is close to constant. This implies that modifying tokenization (and thus compression rate) changes the compute optimal relation between tokens and parameters, whereas the relationship between bytes and parameters remains constant. Therefore, the latter is a more robust way to express the optimal data-to-model-size ratio, and we recommend considering it when designing language models with different tokenizers or vocabularies.

Plotting the values of $B^\star$ and $N^\star$ in Figure 4, across C and T, we observe a log-log linear relationship proving the adequacy of the power law form in Equation 1. The fit reveals the following values of parameters: $B_0 = 17.5$, $N_0 = 9.5 \times 10^{-3}$, $\alpha = 0.465$, $\beta = 0.471$. Crucially, both the values of α and β are close to 0.5, indicating that the optimal byte-per-parameter ratio is close to constant across varying compute budget and compression rates. This allows us to answer the first research question **R1**:

Finding 1

The optimal ratio between bytes of data and model parameters ($\rho^\star$) remains close to constant across variable compute budget and compression rates. Therefore, when generalizing a scaling recipe to a model with a different tokenizer, we advise matching the ratio of training bytes (not tokens) to model parameters.

3.3 Scaling Law II: Optimal Loss Dynamics

In the next stage, we model the optimal loss $L^\star$, defined as the loss obtained with the optimal data $B^\star$ and parameter count $N^\star$ for a given compute budget and compression rate:

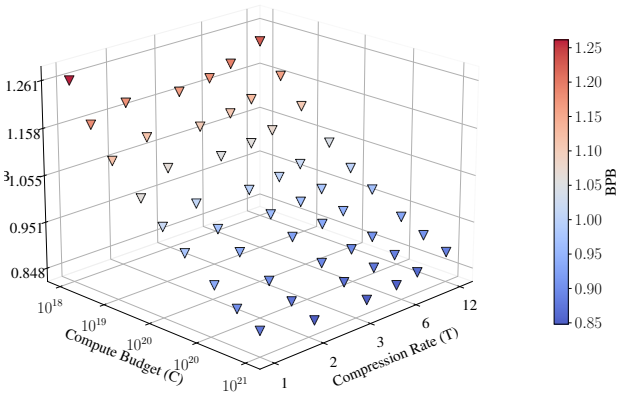

Figure 5 Optimal loss obtained for each compute budget and compression rate with latently tokenized models. Points at $C = 10^{20}$ correspond to the red triangles from Figure 3.

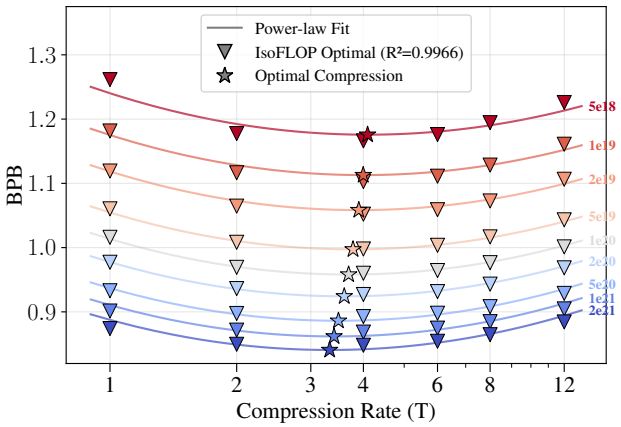

Figure 6 Power law fit for loss prediction based on compute budget and compression rate for BLT models. The slices of the fitted manifold for each compute budget (lines) are compared with the optimal loss values (triangles).

$$L^\star(C,T) \stackrel{\text{def}}{=} L(B^\star(C,T), N^\star(C,T)) \tag{5}$$

We posit that the optimal loss can be approximated by a power law of the form:

$$L^\star(C,T) \cong L_0 \times C^\gamma + f(C,T) \tag{6}$$

This stage involves fitting three variables: L_0 (initial loss), $\gamma < 0$ (scaling with compute), and $f(T)$ (a function representing compression-specific residuals, including irreducible loss). We do not make a priori assumptions about the form of $f(C,T)$; instead, we fit it empirically based on the results obtained for each compression rate separately.

3.4 Scaling Law II: Results

We plot the optimal loss $L^\star$ as a function of compute budget C and compression rate T in Figure 5. While expectedly, the loss decreases with increasing compute budget, we observe that the relation between compression rate T and $L^\star$ is non-monotonic. Specifically, the loss obtains a minimum for $T^\star \approx 4$ and rises for both higher and lower compression rates. We observe a slow decrease of optimal compression rate with increase of compute budget.

The power law fit gives us the following values of parameters: $L_0 = 3342$, $\gamma = -0.206$. We further examine the distribution of compression-specific offsets $f(C,T)$ in Figures 5 and 6. Based on the polynomial profile for $f(\cdot)$ we can estimate with high confidence its form as:[5]

$$f(C,T) = F \times \log^2\left(\frac{C^\delta T}{T_0}\right) + E \tag{7}$$

The best fit was obtained with $F = 0.032$, $\delta = 0.035$, $T_0 = 18.2$, and $E = 0.70$. Both visual and power law evidence support the claim that the optimal compression rate $T^\star = \frac{T_0}{C^\delta}$ slowly decreases with training budget, e.g. $T^\star = 3.69$ for $C = 10^{20}$ and $T^\star = 3.33$ for $C = 2 \times 10^{21}$. This allows us to answer the second research question **R2**:

[5]We discuss empirical derivation of this formula in Appendix B.3.

Parameter	Latent	Subword	95% CI
α	0.465	0.501	[0.471, 0.532]
β	0.471	0.446	[0.387, 0.506]
B_0	17.5	2.8	[0.7, 11.0]
N_0	0.0095	0.059	[0.015, 0.229]
γ	-0.206	-0.181	[-0.226, -0.1352]
L_0	3342	1087	[171, 6896]

Table 1 Fitted power law parameters for the families of latent and subword tokenized models. The 95% confidence intervals were computed with numeric Hessian for the subword tokenized models.

Finding 2

At each training compute budget, there is an optimal compression rate $T^\star$. Diverging from its value in either direction increases loss. We observe decreasing optimal compression rate for higher training budgets.

3.5 Optimal Tokenization during Inference

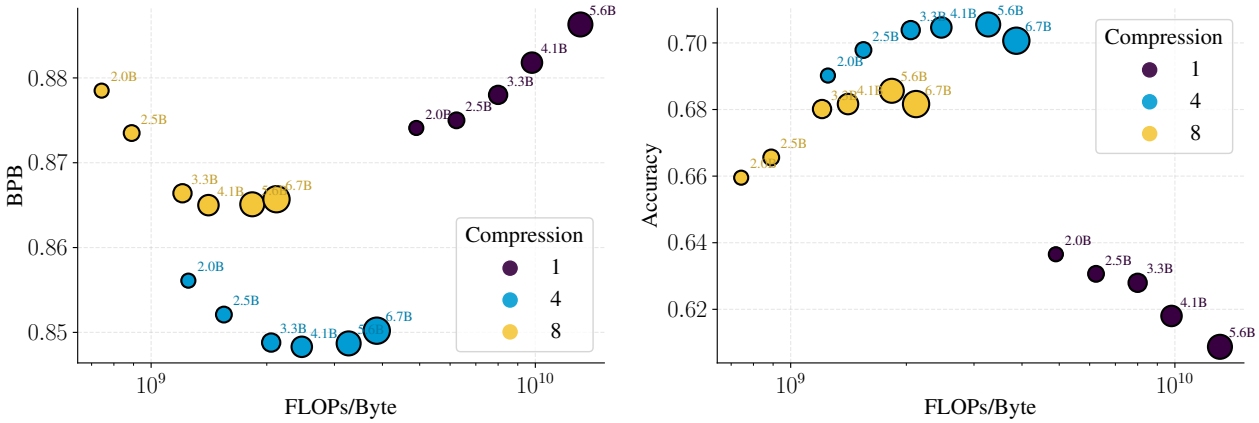

(a) BPB on C4 test-set

(b) 0-shot Accuracy on HellaSwag

Figure 7 Evaluation of the BLT models trained for $C = 2 \times 10^{21}$ FLOPs. Size of the point corresponds to model parameter count in the model. The results are plotted against inference compute cost per byte, which depends on model size N and compression rate T.

To further study the role of optimal tokenization in inference, we compare the performance of models trained under $C = 2 \times 10^{21}$ budget with different compression rates against their inference cost. Specifically, we consider the results on language modeling and 0-shot accuracy on HellaSwag generative benchmark (Zellers et al., 2019). In Figure 7b, we observe that a higher compression rate decreases the inference compute cost for models of the same size (e.g. 3.3B parameter model with $T = 8$ is cheaper to run than a model of the same size $T = 4$). However, we also observe that compression rate closer to the optimal value improves the results of the inference-compute-matched setting. For instance, the 3.3B model with compression rate $T = 4$ has a similar inference cost of 2.1×10^9 FLOPs/Byte as the 6.7B model with compression rate $T = 8$, while the former achieves higher score on the endtask accuracy (74.1% vs. 68.2%). We present further results for AI2 Reasoning Challenge (Clark et al., 2018) in Appendix F.6.

4 Compute Optimal Subword Tokenization

In this section, we validate the observations from the previous section for subword tokenized models. We train models with different subword tokenization algorithms: character-level tokenization, BPE, BPE with vocabulary masking, and SuperBPE to differentiate the values of compression rate T. Then we repeat the analysis of optimal data and parameters configurations and compare the fits of Scaling Laws I and II between latent and subword tokenized models, in order to answer the last research question **R3**.

4.1 Results

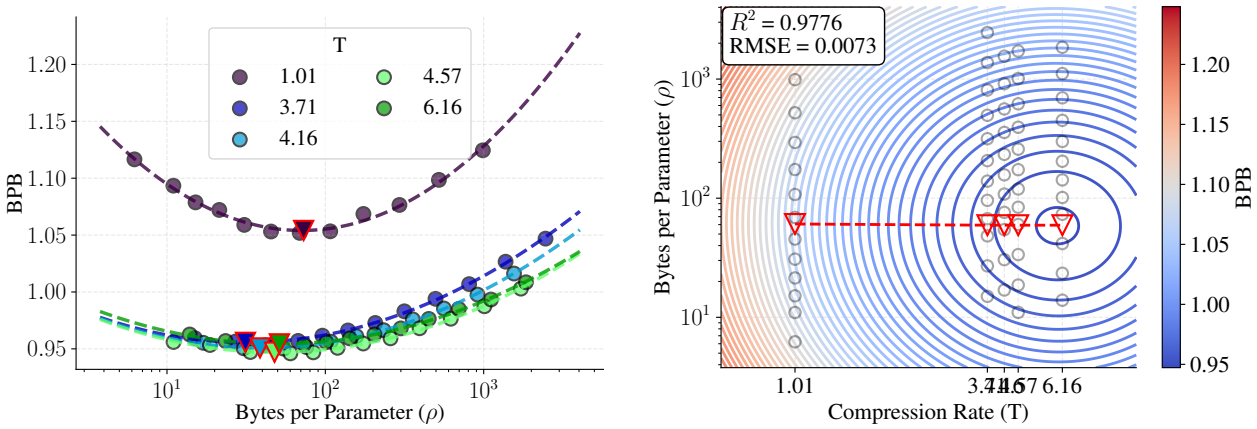

(a) 2D IsoFLOP **(b)** 3D IsoFLOP (heatmap)

Figure 8 Evaluation scores of subword tokenized models on C4 test set with fixed FLOPs budget ($C = 10^{20}$), compared against bytes per parameter ratio. Different subword tokenization algorithms are obtain varying compression rates: 1.01 for character-level tokenization, 3.71, 4.16, and 4.57 for BPE, 6.16 for SuperBPE 2-dimensional IsoFLOP (parabola) were fitted for each compression rate, while 3-dimensional IsoFLOP jointly for all compression rates (on x-axis). Similar to latent tokenized models, minima of both fits show that minimal loss is obtained at almost constant value. For IsoFLOPs as function of data, parameters, and for other compute budgets, refer to Appendix F.1

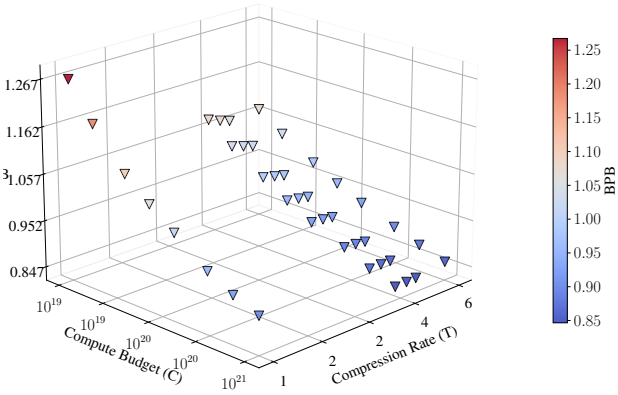

Figure 9 Optimal loss obtained for each compute budget and compression rate. Points at $C = 10^{20}$ correspond to data red triangles from Figure 8.

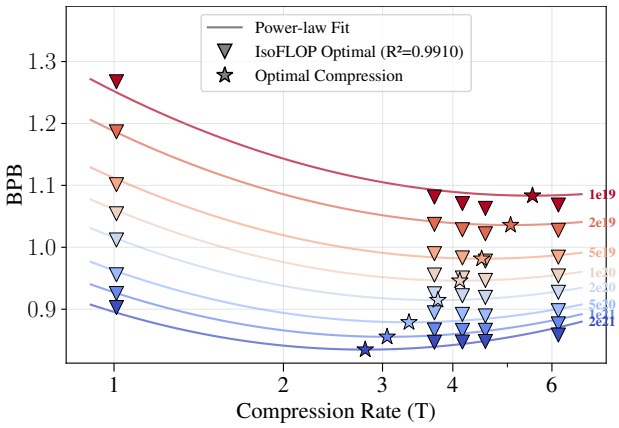

Figure 10 Power law fit for loss prediction based on compute budget and compression rate for isotropic models. The slices of the fitted manifold for each compute budget (lines) are compared with the optimal loss values (triangles).

Similar to the latent tokenization case, the IsoFLOPs curves allow us to identify the optimal data amount in bytes $B^\star$ for a fixed compute budget C. Figure 8 shows the optimal values for a specific compute budget. We observe that the optimal byte-per-parameter ratio $\rho^\star$ is similar across tokenizers.

Compute (FLOPs)	Character	BPE			SuperBPE
		V. mask=90%	V. mask=75%	Original	
1×10^{19}	1.2678	1.0819	1.0709	**1.0635**	1.0682
2×10^{19}	1.1812	1.0381	1.0281	**1.0214**	1.0273
5×10^{19}	1.0989	0.9887	0.9819	**0.9769**	0.9840
1×10^{20}	1.0519	0.9554	0.9502	**0.9461**	0.9532
2×10^{20}	1.0126	0.9254	0.9220	**0.9186**	0.9272
5×10^{20}	0.9556	0.8942	0.8916	**0.8891**	0.8976
1×10^{21}	0.9253	0.8665	**0.8658**	0.8659	0.8763
2×10^{21}	0.9027	**0.8466**	0.8469	0.8479	0.8582
Compression:	1.01	3.71	4.16	4.57	6.16

Table 2 Comparison of the lowest BPB obtained by subword tokenized models for specific compute budgets.

The Scaling Law I fit shows results close to the latent tokenization case: $B_0 = 2.8$, $N_0 = 59 \times 10^{-3}$, $\alpha = 0.501$, $\beta = 0.446$. Also, loss dynamics presented in Figure 9 and the Scaling Law II fit show similar results as the latent tokenization case: $L_0 = 1087$, $\gamma = -0.181$, $F = 0.0575$, $\delta = 0.129$, $T_0 = 1577$, and $E = 0.680$. The fit values are compared with latent tokenized models, as shown in Table 1.

Similar to last section, we observe the presence of compute optimal compression rate that decrease for higher compute budgets (Figure 10). Surprisingly, under a high compute budget, the models with 90% and 75% of vocabulary masked (yet still included in FLOPs computation) outperform the models with original BPE tokenizers, as shown in Table 2. It empirically shows that lower compression is beneficial for training of larger scale models.

These observations allow us to answer the question **R3**:

Finding 3

Discovered scaling trends for models with latent tokenization (BLT) hold for models with subword tokenization (BPE, SuperBPE).

5 Compute Optimal Tokenization Beyond English

To test how the language choice affects the compute-optimal compression rate and bytes per parameter ratio, we extend our experiments to five languages with diverse writing scripts: French (Latin), Vietnamese (Latin), Russian (Cyrillic), Arabic (Arabic), Hindi (Devanagari). We also create an artificially inflated version of English data by adding a dummy byte between pairs of original UTF-8 bytes. Such English $\times 2$ data represent the same information at half the density.

For this purpose, we train latent-tokenized models (BLT) on monolingual data from FineWeb-2 (Penedo et al., 2025), training a separate set of models for each language.[6] We evaluate each model on the corresponding test split from the same source. For English $\times 2$, we use an inflated version of the C4 test set used in the previous experiments.

Our training setup is analogous to the one described in Section 3 for English. For each language l, we fix the training budget to $C = 10^{20}$ FLOPs. The IsoFLOPs analysis (similar to that presented in Figure 3) allows us to identify the compute optimal bytes per parameter ratio $\rho_l^\star$ and compression rate $T_l^\star$, for each language l at fixed compute budget.

[6]The results for jointly trained multilingual models are in Appendix D).

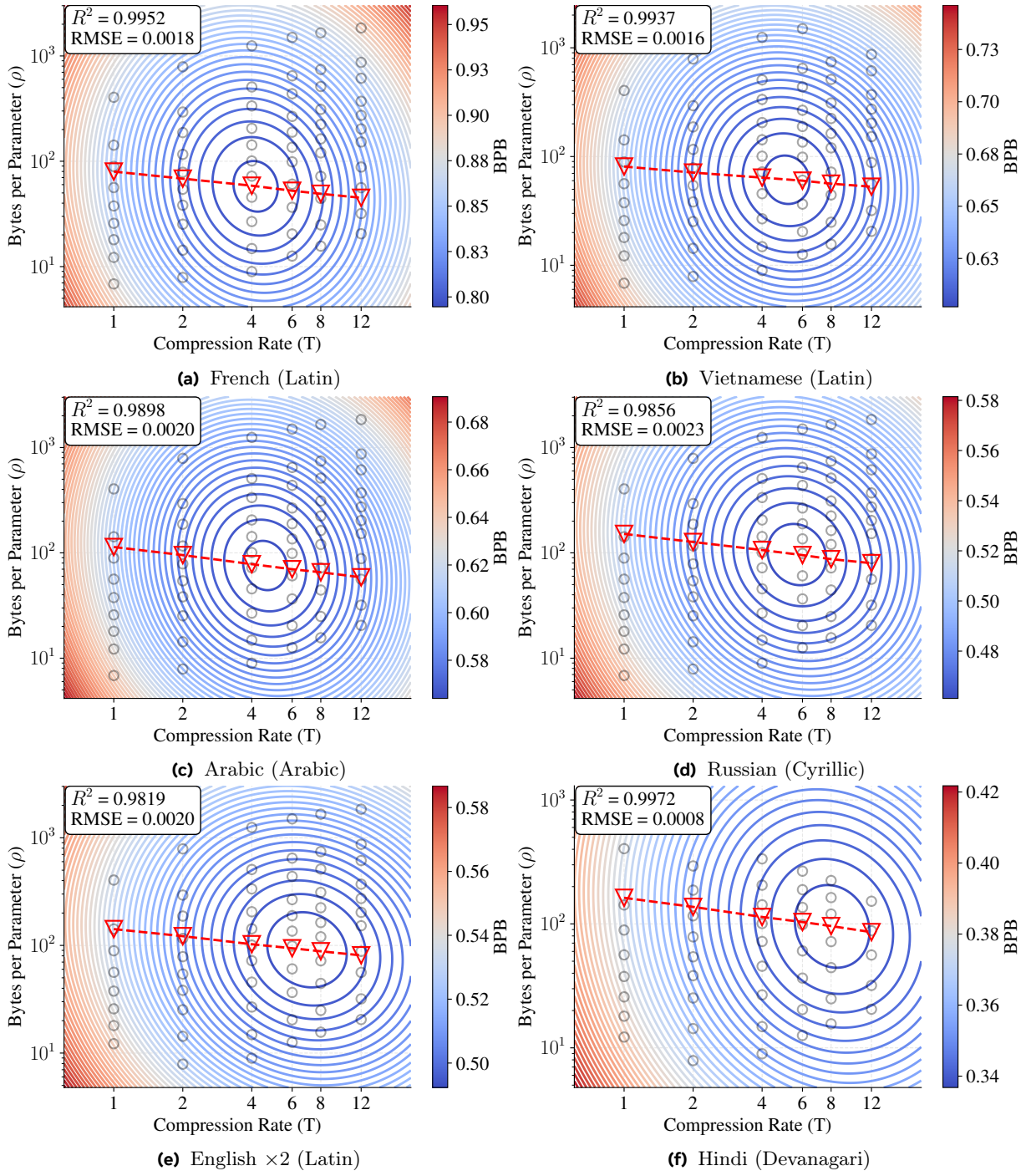

Figure 11 3D IsoFLOP (heatmap) fits across languages ($C = 10^{20}$) as function of bytes per parameter and compression rate for six languages. All models use latent tokenization to achieve the set compression. IsoFLOPs are fitted jointly for all compression rates.

Further, we compare these values to cross-lingual parity, defined as the proportion between the amount of bytes required to express the same information in different languages (Petrov et al., 2023). We estimate parity by dividing the byte length of sentences in each language by the byte length of their English translations. We use translations from FLORES-200 multi-parallel corpus (Goyal et al., 2021; team et al., 2022), which test split contains 1000 English sentences and their translations in a wide range of languages.

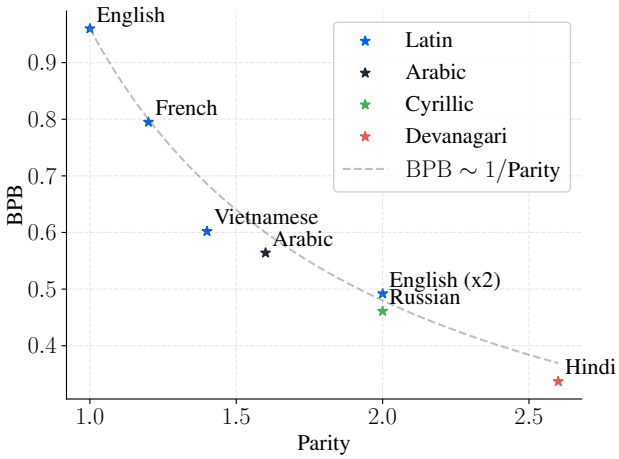

Figure 12 Language specific minimal loss compared against parity. We observe that BPB is inversely proportional to parity.

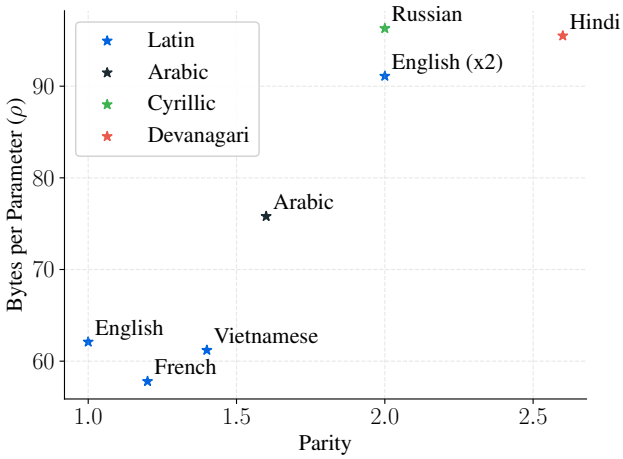

Figure 13 Language specific optimal bytes per parameter ratio ($\rho_l^\star$). Lower information density (high parity) correlates with preference of large training data size over model size (high $\rho_l^\star$).

Language	Parity	$\rho_l^\star$		$T_l^\star$		BPB
		Value	Ratio	Value	Ratio	
English	1.0	62.1	1.0	3.71	1.0	0.960
French	1.2	57.8	0.93	4.16	1.12	0.795
Vietnamese	1.4	61.2	0.99	5.11	1.38	0.602
Arabic	1.6	75.8	1.22	4.58	1.23	0.564
Russian	2.0	96.3	1.55	5.67	1.52	0.461
English (x2)	2.0	91.1	1.47	6.97	1.87	0.492
Hindi	2.6	95.5	1.54	8.09	2.18	0.337

Table 3 Compute-optimal byte-per-parameter ($\rho_l^\star$), compression rate ($T_l^\star$) compared to cross-lingual parity. Results for monolingual models, with $C = 10^{20}$ FLOPs budget. The parity and compute-optimal ratios are proportions between each language and English baseline.

These experiments address our last research question **R4**.

5.1 Results

Figures 24 and 11 present the results of the IsoFLOPs analysis across all analyzed languages. Similarly to English, we observe that the minimal loss is achieved by models with close to constant bytes per parameter ($\rho_l^\star$). From the polynomial fit, we estimate the compute-optimal bytes per parameter ratio and compression rate by analytically finding the coordinates of the global minimum (i.e. lowest loss).

Notably, the $\rho_l^\star$ is language dependent (e.g. $\rho_{\text{AR}}^\star \approx 75.8$; $\rho_{\text{RU}}^\star \approx 96.3$). We also observe language-dependent differences in the compute-optimal compression rate (e.g. $T_{\text{AR}}^\star \approx 4.58$; $T_{\text{RU}}^\star \approx 5.67$). In Table 3, we compare these compute-optimal values to cross-lingual parity. We observe that the optimal values depend on language and its parity. Figure 12 shows that language-specific BPB scales inversely with parity. This confirms the observation from Limisiewicz et al. (2024): under optimal tokenization, similar information expressed across languages has similar likelihood. We further observe that parity correlates with optimal bytes per parameter, which is explained by the fact that more coarsely encoded languages tend to benefit more from additional training data than from larger models (Figure 13). While, in joint multilingual training the optimal bytes per parameter ratios converge to the same value across languages (see Appendix D).

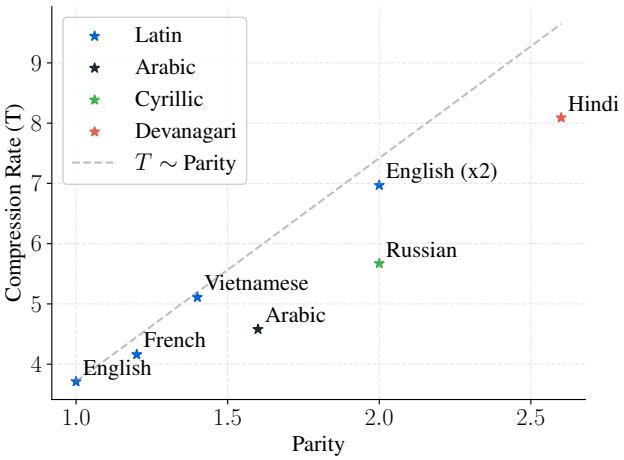

Figure 14 Language specific compression rate ($T_l^\star$) compared against parity. We observe that languages with higher parity prefer tokenization with higher compression.

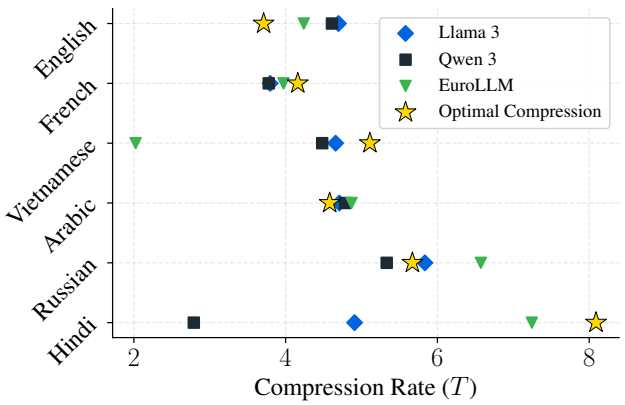

Figure 15 Compute optimal compression differs from the data compression obtained by popular language models. We observe that popular pre-trained subword tokenizers tend to over-compress high-resource languages, e.g.: English, Arabic, while significantly undercompressing the less resourced ones, e.g.: Vietnamese, Hindi.

Lastly, we observe that higher parity translates to a higher optimal compression rate. For Latin-script languages, this relationship is close to a 1:1 increase (Figure 14). Importantly, the compression achieved by popular multilingual tokenizers: Llama 3 (Llama Team, AI @ Meta, 2024), Qwen 3 (Team, 2025), and EuroLLM (Martins et al., 2025), differs from the optimal value, as seen in Figure 15. These tokenizers tend to over-compress high-resource languages while under-compressing lower-resource ones.

These results bring an answer to the last research question **[R4]**:

Finding 4

The optimal byte of data to parameter ratio ($\rho^\star$) and compression rate ($T^\star$) vary across different languages. Both are correlated with average information value of bytes in a given language (measured by parity).

6 Related Work

6.1 Data Compression in Scaling Laws

Foundational studies on neural scaling laws, such as those by Kaplan et al. (2020) and Hoffmann et al. (2022), have primarily focused on the relationship between model size, dataset size (in tokens), and compute. Subsequent works (Pearce and Song, 2024; Porian et al., 2024) have pointed out that the decision of whether to include vocabulary embeddings in the analysis was one of the causes of divergence between scaling laws derived in these studies. Hoffmann et al. (2022) propose a compute-optimal training ratio of approximately 20 tokens per parameter. However, they assume a fixed tokenization scheme, overlooking the information content of the tokens themselves. We generalize this scaling rule across tokenizers and express it as a comprehensive byte-per-parameter ratio: $\rho^\star \approx 60$ (for English data).

Tao et al. (2024) derived scaling laws for vocabulary size in BPE-tokenized models. Their study explores how varying vocabulary size impacts computational cost and performance. They also consider the importance of compression rate in model scaling, which is indirectly controlled by the vocabulary size. By considering a broad scope of compression values and compute budgets, we show that the benefits of scaling up vocabulary diminish at larger scales. We further discuss differences between experimental settings in Appendix E.

Multiple recent works discussed language model scaling trends across domains and languages. Yang et al. (2025) derived scaling laws across programming languages, showing that language-specific data composition

significantly affects scaling behavior. In the multilingual space, He et al. (2025) established per-language scaling laws, while Longpre et al. (2026) studied the dynamics of cross-lingual transfer at scale. Overall, these works demonstrate that scaling laws differ across domains and languages, as we have also observed in our multilingual experiments.

6.2 Search for Optimal Tokenization

The research community has long sought to identify tokenizer properties that correlate with language model performance. The compression rate, or its proxies such as *fertility*, have been identified as a significant factor, especially in the multilingual setting. Rust et al. (2021) observed that in multilingual language models, monolingual tokenizers with higher in-language compression outperform multilingual ones. Similarly, Limisiewicz et al. (2023); Goldman et al. (2024) noted the benefits of higher compression rate for certain downstream tasks in multilingual models. Gallé (2019) show that higher compression is also beneficial for machine translation. However, in the subword tokenizers considered in these works, language-specific compression depends on the representation of the language in the training corpora. Thus, compression could be a proxy for the root cause of the performance differences, namely language frequency in the data mix.

In monolingual (English) models, Schmidt et al. (2024) argued that higher compression is not inherently beneficial. However, Liu et al. (2025) observed an upward trend in downstream task performance with higher compression, even when perplexity (measured in bits per byte) degraded. This discrepancy underscores the importance of evaluating downstream performance alongside language modeling metrics.

In contrast to prior work, our extensive search reveals that the impact of compression rate on performance is non-monotonic: there exists an optimal compression rate beyond which performance degrades. We also observe a preference for lower compression in longer training. The recurring prior-work assumption linking higher compression rate with performance improvement in the multilingual setting may stem from the fact that subword tokenizers typically result in a lower-than-optimal compression rate for low-resource languages, as shown in Figure 15.

6.3 Scaling Latent Tokenized Models

We employ BLT (Pagnoni et al., 2025) as our primary framework for studying scaling laws with variable compression. Techniques such as entropy-based or static patching allow precise control of the compression rate across a wide range. While promising, the data efficiency of training and inference for dynamically tokenized models has not yet been comprehensively studied in the context of scaling laws.

Recent results in latent tokenization suggest that this approach yields greater gains at scale. The works of Pagnoni et al. (2025); Hwang et al. (2025); Neitemeier et al. (2025); Nawrot et al. (2023) demonstrate that, given sufficient training compute, hierarchical models can surpass their subword-tokenized counterparts. Furthermore, latent tokenization allows adjusting compression for specific languages (Ahia et al., 2024; Owodunni et al., 2025). Based on our findings, we expect such approaches to be particularly beneficial for multilingual language modeling.

7 Discussion

The relationship between scaling laws and data compression highlights the importance of considering tokenizer compression rate in the optimal design of large language models. Our observations overlap with the Hoffmann et al. (2022) (Chinchilla) recipe, suggesting that data and model parameters should be scaled proportionally. Generalizing the Chinchilla rule, we show that the appropriate unit for data quantity is bytes, not tokens. Therefore, the widely accepted rule of using approximately 20 tokens per parameter for compute-optimal training holds only under compression rate specific to a BPE tokenizer. We generalize this rule (Scaling Law I) by empirically showing that compute-optimal architectures for English text should use approximately 60 bytes per parameter, regardless of data compression. This generalization makes it easy to transfer efficient training settings across different tokenization schemes, spanning from byte-level to superword-level tokens.

Furthermore, Scaling Law II reveals the existence of an optimal compression rate that depends on the training

domain and the compute budget. Interestingly, when training on English data with a small FLOP budget, the optimal compression rate is close to that of a BPE tokenizer. However, we observe a slow decrease as training compute increases. This observation also holds for subword-tokenized models. Strikingly, a model with 90% of the BPE vocabulary masked performs slightly better than standard BPE in our largest runs (even though both spend the same compute in the embedding and de-embedding layers). This surprising result suggests that, for compute-efficient training of large models, it could be beneficial to decrease vocabulary size or apply techniques such as BPE-dropout (Provilkov et al., 2020). Why do we observe such a counterintuitive result? Our hypothesis is that less-compressed tokenizers allow the model to use more compute at inference time by dividing each evaluation sample into more tokens that are processed by the model. It is important to keep in mind that lower compression naturally increases the cost of model usage (as shown in Section 3.5). Therefore, when controlling for compression rate, we should consider the trade-off between performance and inference cost. Specifically, it is advisable to use higher compression rate to decrease model usage cost, similarly to how model developers opt for over-training language models to boost the performance of relatively smaller (and thus cheaper) models compared to their training-compute-optimal counterparts.

The search for compute-optimal compression rate is especially important for languages other than English, where the compression obtained by subword tokenizers tends to diverge from the optimal value to a more extreme extent. Previously, it was thought that multilingual performance of language models is affected by over-segmentation, and many studies focused on increasing compression for better multilingual performance (Rust et al., 2021; Limisiewicz et al., 2023). We observe, across all considered languages, that overly high compression deteriorates results. Furthermore, for each language we find a specific optimal compression rate, the value of which is correlated with the relative information density of the text, i.e., *parity*. This observation highlights the importance of identifying and achieving an optimal compression rate for each of the modeled languages. For statistics-based subword tokenizers (such as BPE), compression rate is heavily impacted by the amount of in-language data in the training corpus (Ahia et al., 2023) and encoding efficiency (Limisiewicz et al., 2024), and thus cannot be easily controlled in a massively multilingual setting. This limitation provides a strong argument for latent tokenizers in multilingual language modeling, whose compression can be adapted for specific languages (Ahia et al., 2024; Owodunni et al., 2025).

7.1 Future Work

While our study is the most comprehensive investigation of the impact of tokenization on scaling laws to date, there are multiple directions for future work in this area:

Optimal Compression for Other Modalities. In this work, we focused on text data. We expect the impact of data compression to be equally relevant for other modalities, such as vision, speech, and code. Currently, each modality utilizes a different set of tokenization techniques, such as variational autoencoders (van den Oord et al., 2017) or vision transformers (Yu et al., 2024) for images. Therefore, the scaling analysis requires considering the impact of modality-specific tokenization artifacts.

Sparse Architectures. Another direction is considering architectures other than dense (hierarchical) transformer models, such as Mixture of Experts (MoE) models. Studying the role of data compression could answer the question of how it interacts with parameter sparsity, and thus could be an important contribution to MoE scaling laws (Ludziejewski et al., 2024).

7.2 Limitations

To keep the study tractable, we fixed several training hyperparameters across all runs. In particular, we did not tune the learning rate for specific training budgets or adapt any hyperparameters other than those named.

While we have examined a wide range of tokenization methods, spanning both latent and subword families, there could be other design choices that affect the results. Examples of such aspects include pre-tokenization rules, other subword algorithms (e.g., Unigram; Kudo, 2018), or token boundary prediction for latent tokenizers. We expect that such changes would have a minor effect on the main findings of this work. In Appendix C, we provide a further comparison across tokenization methods.

8 Conclusion

In this work, we have systematically studied the role of data compression on the scaling trend for large language models. We have shown that the optimal ratio between training data bytes and model parameters, denoted as $\rho^\star$, remains approximately constant across varying compute budgets and compression rates. Consequently, when generalizing scaling recipes to models with different tokenizers, we advise matching the ratio of training bytes (not tokens) to model parameters. Additionally, we find the optimal compression rate $T^\star$ that is specific to the training domain and slowly decreases with the training budget. Finally, we show that these scaling trends with compression rate hold consistently for both latent and subword-tokenized models.

Acknowledgments

We thank Jonathan Hayase, Julie Kallini, Pedro Rodriguez, and Rylan Schaeffer for insightful discussions that helped shape and improve this work. We are grateful to Artyom Kozhevnikov, David Dale, and Marta R. Costa-jussà for their advice and practical assistance with multilingual experiments. Finally, we express special gratitude to Cody Ohlsen for going to great lengths to resolve technical obstacles at one of the project's most critical moments.

References

Orevaoghene Ahia, Sachin Kumar, Hila Gonen, Jungo Kasai, David Mortensen, Noah Smith, and Yulia Tsvetkov. Do all languages cost the same? tokenization in the era of commercial language models. In Houda Bouamor, Juan Pino, and Kalika Bali, editors, *Proceedings of the 2023 Conference on Empirical Methods in Natural Language Processing*, pages 9904–9923, Singapore, December 2023. Association for Computational Linguistics. doi: 10.18653/v1/2023.emnlp-main.614. https://aclanthology.org/2023.emnlp-main.614/.

Orevaoghene Ahia, Sachin Kumar, Hila Gonen, Valentin Hofmann, Tomasz Limisiewicz, Yulia Tsvetkov, and Noah A Smith. Magnet: Improving the multilingual fairness of language models with adaptive gradient-based tokenization. In A. Globerson, L. Mackey, D. Belgrave, A. Fan, U. Paquet, J. Tomczak, and C. Zhang, editors, *Advances in Neural Information Processing Systems*, volume 37, pages 47790–47814. Curran Associates, Inc., 2024. doi: 10.52202/079017-1514. https://proceedings.neurips.cc/paper_files/paper/2024/file/5572bc595de865c1450868fd5391e9c5-Paper-Conference.pdf.

Peter Clark, Isaac Cowhey, Oren Etzioni, Tushar Khot, Ashish Sabharwal, Carissa Schoenick, and Oyvind Tafjord. Think you have solved question answering? try arc, the ai2 reasoning challenge. *arXiv:1803.05457v1*, 2018.

Matthias Gallé. Investigating the effectiveness of BPE: The power of shorter sequences. In Kentaro Inui, Jing Jiang, Vincent Ng, and Xiaojun Wan, editors, *Proceedings of the 2019 Conference on Empirical Methods in Natural Language Processing and the 9th International Joint Conference on Natural Language Processing (EMNLP-IJCNLP)*, pages 1375–1381, Hong Kong, China, November 2019. Association for Computational Linguistics. doi: 10.18653/v1/D19-1141. https://aclanthology.org/D19-1141/.

Omer Goldman, Avi Caciularu, Matan Eyal, Kris Cao, Idan Szpektor, and Reut Tsarfaty. Unpacking tokenization: Evaluating text compression and its correlation with model performance. In Lun-Wei Ku, Andre Martins, and Vivek Srikumar, editors, *Findings of the Association for Computational Linguistics: ACL 2024*, pages 2274–2286, Bangkok, Thailand, August 2024. Association for Computational Linguistics. doi: 10.18653/v1/2024.findings-acl.134. https://aclanthology.org/2024.findings-acl.134/.

Naman Goyal, Cynthia Gao, Vishrav Chaudhary, Peng-Jen Chen, Guillaume Wenzek, Da Ju, Sanjana Krishnan, Marc'Aurelio Ranzato, Francisco (Paco) Guzmán, and Angela Fan. The flores-101 evaluation benchmark for low-resource and multilingual machine translation. *Transactions of the Association for Computational Linguistics*, 10:522–538, 2021. https://https://arxiv.org/abs/2106.03193.

Yifei He, Alon Benhaim, Barun Patra, Praneetha Vaddamanu, Sanchit Ahuja, Parul Chopra, Vishrav Chaudhary, Han Zhao, and Xia Song. Scaling laws for multilingual language models. In Wanxiang Che, Joyce Nabende, Ekaterina Shutova, and Mohammad Taher Pilehvar, editors, *Findings of the Association for Computational Linguistics: ACL 2025*, pages 4257–4273, Vienna, Austria, July 2025. Association for Computational Linguistics. ISBN 979-8-89176-256-5. doi: 10.18653/v1/2025.findings-acl.221. https://aclanthology.org/2025.findings-acl.221/.

Jordan Hoffmann, Sebastian Borgeaud, Arthur Mensch, Elena Buchatskaya, Trevor Cai, Eliza Rutherford, Diego de Las Casas, Lisa Anne Hendricks, Johannes Welbl, Aidan Clark, Tom Hennigan, Eric Noland, Katie Millican, George van den Driessche, Bogdan Damoc, Aurelia Guy, Simon Osindero, Karen Simonyan, Erich Elsen, Jack W. Rae, Oriol Vinyals, and Laurent Sifre. Training compute-optimal large language models. *arXiv preprint arXiv:2203.15556*, 2022. https://arxiv.org/abs/2203.15556.

Sukjun Hwang, Brandon Wang, and Albert Gu. Dynamic chunking for end-to-end hierarchical sequence modeling, 2025. https://arxiv.org/abs/2507.07955.

Jared Kaplan, Sam McCandlish, Tom Henighan, Tom B. Brown, Benjamin Chess, Rewon Child, Scott Gray, Alec Radford, Jeffrey Wu, and Dario Amodei. Scaling laws for neural language models. *arXiv preprint arXiv:2001.08361*, 2020. https://arxiv.org/abs/2001.08361.

Taku Kudo. Subword regularization: Improving neural network translation models with multiple subword candidates. In Iryna Gurevych and Yusuke Miyao, editors, *Proceedings of the 56th Annual Meeting of the Association for Computational Linguistics (Volume 1: Long Papers)*, pages 66–75, Melbourne, Australia, July 2018. Association for Computational Linguistics. doi: 10.18653/v1/P18-1007. https://aclanthology.org/P18-1007/.

Jeffrey Li, Alex Fang, Georgios Smez, Alon Albalak, Kaber Mehta, Etash Openshaw, Louis Haber, Mitchell Wortsman, Sedrick Keh, Samir Yitzhak Gadre, Rohan Taori, Shuran Tian, Jenia Jitsev, Gabriel Ilharco, Alexander Smola, Ali Farhadi, Vaishaal Shankar, Ludwig Schmidt, Yair Carmon, and Romain Beaumont. Datacomp-lm: In search of the next generation of training sets for language models. *arXiv preprint arXiv:2406.11794*, 2024. https://arxiv.org/abs/2406.11794.

Margaret Li, Sneha Kudugunta, and Luke Zettlemoyer. (mis)fitting scaling laws: A survey of scaling law fitting techniques in deep learning. In *The Thirteenth International Conference on Learning Representations*, 2025. https://openreview.net/forum?id=xI71dsS3o4.

Tomasz Limisiewicz, Jiří Balhar, and David Mareček. Tokenization impacts multilingual language modeling: Assessing vocabulary allocation and overlap across languages. In Anna Rogers, Jordan Boyd-Graber, and Naoaki Okazaki, editors, *Findings of the Association for Computational Linguistics: ACL 2023*, pages 5661–5681, Toronto, Canada, July 2023. Association for Computational Linguistics. doi: 10.18653/v1/2023.findings-acl.350. https://aclanthology.org/2023.findings-acl.350/.

Tomasz Limisiewicz, Terra Blevins, Hila Gonen, Orevaoghene Ahia, and Luke Zettlemoyer. MYTE: Morphology-driven byte encoding for better and fairer multilingual language modeling. In Lun-Wei Ku, Andre Martins, and Vivek Srikumar, editors, *Proceedings of the 62nd Annual Meeting of the Association for Computational Linguistics (Volume 1: Long Papers)*, pages 15059–15076, Bangkok, Thailand, August 2024. Association for Computational Linguistics. doi: 10.18653/v1/2024.acl-long.804. https://aclanthology.org/2024.acl-long.804/.

Alisa Liu, Jonathan Hayase, Valentin Hofmann, Sewoong Oh, Noah A. Smith, and Yejin Choi. Superbpe: Space travel for language models, 2025. https://arxiv.org/abs/2503.13423.

Dong C. Liu and Jorge Nocedal. On the limited memory bfgs method for large scale optimization. *Math. Program.*, 45 (1–3):503–528, August 1989. ISSN 0025-5610.

Llama Team, AI @ Meta. The llama 3 herd of models. *arXiv preprint arXiv:2407.21783*, 2024. https://arxiv.org/abs/2407.21783.

Shayne Longpre, Sneha Kudugunta, Niklas Muennighoff, I-Hung Hsu, Isaac Caswell, Alex Pentland, Sercan Arik, Chen-Yu Lee, and Sayna Ebrahimi. Atlas: Adaptive transfer scaling laws for multilingual pretraining, finetuning, and decoding the curse of multilinguality, 2026. https://arxiv.org/abs/2510.22037.

Ilya Loshchilov and Frank Hutter. Decoupled weight decay regularization. 2019. https://arxiv.org/abs/1711.05101.

Jan Ludziejewski, Jakub Krajewski, Kamil Adamczewski, Maciej Pióro, Michał Krutul, Szymon Antoniak, Kamil Ciebiera, Krystian Król, Tomasz Odrzygóźdź, Piotr Sankowski, Marek Cygan, and Sebastian Jaszczur. Scaling laws for fine-grained mixture of experts. In Ruslan Salakhutdinov, Zico Kolter, Katherine Heller, Adrian Weller, Nuria Oliver, Jonathan Scarlett, and Felix Berkenkamp, editors, *Proceedings of the 41st International Conference on Machine Learning*, volume 235 of *Proceedings of Machine Learning Research*, pages 33270–33288. PMLR, 21–27 Jul 2024. https://proceedings.mlr.press/v235/ludziejewski24a.html.

Pedro Henrique Martins, Patrick Fernandes, João Alves, Nuno M. Guerreiro, Ricardo Rei, Duarte M. Alves, José Pombal, Amin Farajian, Manuel Faysse, Mateusz Klimaszewski, Pierre Colombo, Barry Haddow, José G.C. de Souza, Alexandra Birch, and André F.T. Martins. Eurollm: Multilingual language models for europe. *Procedia Comput. Sci.*, 255(C):53–62, January 2025. ISSN 1877-0509. doi: 10.1016/j.procs.2025.02.260. https://doi.org/10.1016/j.procs.2025.02.260.

Piotr Nawrot, Jan Chorowski, Adrian Lancucki, and Edoardo Maria Ponti. Efficient transformers with dynamic token pooling. In Anna Rogers, Jordan Boyd-Graber, and Naoaki Okazaki, editors, *Proceedings of the 61st Annual Meeting of the Association for Computational Linguistics (Volume 1: Long Papers)*, pages 6403–6417, Toronto, Canada, July 2023. Association for Computational Linguistics. doi: 10.18653/v1/2023.acl-long.353. https://aclanthology.org/2023.acl-long.353/.

Pit Neitemeier, Björn Deiseroth, Constantin Eichenberg, and Lukas Balles. Hierarchical autoregressive transformers: Combining byte- and word-level processing for robust, adaptable language models. In *The Thirteenth International Conference on Learning Representations*, 2025. https://openreview.net/forum?id=tU074jg2vS.

Abraham Toluase Owodunni, Orevaoghene Ahia, and Sachin Kumar. Flexitokens: Flexible tokenization for evolving language models. *arXiv preprint arXiv:2507.12720*, 2025.

Artidoro Pagnoni, Ramakanth Pasunuru, Pedro Rodriguez, John Nguyen, Benjamin Muller, Margaret Li, Chunting Zhou, Lili Yu, Jason E Weston, Luke Zettlemoyer, Gargi Ghosh, Mike Lewis, Ari Holtzman, and Srini Iyer. Byte latent transformer: Patches scale better than tokens. In *Proceedings of the 63rd Annual Meeting of the Association for Computational Linguistics (Volume 1: Long Papers)*, pages 9238–9258, Vienna, Austria, July 2025. Association for Computational Linguistics. doi: 10.18653/v1/2025.acl-long.453. https://aclanthology.org/2025.acl-long.453/.

Tim Pearce and Jinyeop Song. Reconciling kaplan and chinchilla scaling laws. In *TMLR*, 2024.

Guilherme Penedo, Hynek Kydlíček, Vinko Sabolčec, Bettina Messmer, Negar Foroutan, Amir Hossein Kargaran, Colin Raffel, Martin Jaggi, Leandro Von Werra, and Thomas Wolf. Fineweb2: One pipeline to scale them all – adapting pre-training data processing to every language, 2025. https://arxiv.org/abs/2506.20920.

Aleksandar Petrov, Emanuele La Malfa, Philip H. S. Torr, and Adel Bibi. Language model tokenizers introduce unfairness between languages. In *Advances in Neural Information Processing Systems*, 2023. https://arxiv.org/abs/2305.15425.

Tomer Porian, Mitchell Wortsman, Jenia Jitsev, Ludwig Schmidt, and Yair Carmon. Resolving discrepancies in compute-optimal scaling of language models. In A. Globerson, L. Mackey, D. Belgrave, A. Fan, U. Paquet, J. Tomczak, and C. Zhang, editors, *Advances in Neural Information Processing Systems*, volume 37, pages 100535–100570. Curran Associates, Inc., 2024. doi: 10.52202/079017-3189. https://proceedings.neurips.cc/paper_files/paper/2024/file/b6341525cd84f3be0ef203e4d7cd8556-Paper-Conference.pdf.

Ivan Provilkov, Dmitrii Emelianenko, and Elena Voita. BPE-dropout: Simple and effective subword regularization. In Dan Jurafsky, Joyce Chai, Natalie Schluter, and Joel Tetreault, editors, *Proceedings of the 58th Annual Meeting of the Association for Computational Linguistics*, pages 1882–1892, Online, July 2020. Association for Computational Linguistics. doi: 10.18653/v1/2020.acl-main.170. https://aclanthology.org/2020.acl-main.170/.

Colin Raffel, Noam Shazeer, Adam Roberts, Katherine Lee, Sharan Narang, Michael Matena, Yanqi Zhou, Wei Li, and Peter J. Liu. Exploring the limits of transfer learning with a unified text-to-text transformer. *Journal of Machine Learning Research*, 21(140):1–67, 2020. http://jmlr.org/papers/v21/20-074.html.

Phillip Rust, Jonas Pfeiffer, Ivan Vulić, Sebastian Ruder, and Iryna Gurevych. How good is your tokenizer? on the monolingual performance of multilingual language models. In Chengqing Zong, Fei Xia, Wenjie Li, and Roberto Navigli, editors, *Proceedings of the 59th Annual Meeting of the Association for Computational Linguistics and the 11th International Joint Conference on Natural Language Processing (Volume 1: Long Papers)*, pages 3118–3135, Online, August 2021. Association for Computational Linguistics. doi: 10.18653/v1/2021.acl-long.243. https://aclanthology.org/2021.acl-long.243/.

Craig W Schmidt, Varshini Reddy, Haoran Zhang, Alec Alameddine, Omri Uzan, Yuval Pinter, and Chris Tanner. Tokenization is more than compression. In Yaser Al-Onaizan, Mohit Bansal, and Yun-Nung Chen, editors, *Proceedings of the 2024 Conference on Empirical Methods in Natural Language Processing*, pages 678–702, Miami, Florida, USA, November 2024. Association for Computational Linguistics. doi: 10.18653/v1/2024.emnlp-main.40. https://aclanthology.org/2024.emnlp-main.40/.

Rico Sennrich, Barry Haddow, and Alexandra Birch. Neural machine translation of rare words with subword units. In *Proceedings of the 54th Annual Meeting of the Association for Computational Linguistics (Volume 1: Long Papers)*, pages 1715–1725, Berlin, Germany, August 2016. Association for Computational Linguistics. doi: 10.18653/v1/P16-1162. https://aclanthology.org/P16-1162/.

Kevin Slagle. Spacebyte: Towards deleting tokenization from large language modeling. In *The Thirty-eighth Annual Conference on Neural Information Processing Systems*, 2024. https://openreview.net/forum?id=KEe4IUp20I.

Chaofan Tao, Qian Liu, Longxu Dou, Niklas Muennighoff, Zhongwei Wan, Ping Luo, Min Lin, and Ngai Wong. Scaling laws with vocabulary: Larger models deserve larger vocabularies. In *The Thirty-eighth Annual Conference on Neural Information Processing Systems*, 2024. https://openreview.net/forum?id=sKCKPr8cRL.

Nllb team, Marta Ruiz Costa-jussà, James Cross, Onur cCelebi, Maha Elbayad, Kenneth Heafield, Kevin Heffernan, Elahe Kalbassi, Janice Lam, Daniel Licht, Jean Maillard, Anna Sun, Skyler Wang, Guillaume Wenzek, Alison Youngblood, Bapi Akula, Loïc Barrault, Gabriel Mejia Gonzalez, Prangthip Hansanti, John Hoffman, Semarley Jarrett, Kaushik Ram Sadagopan, Dirk Rowe, Shannon L. Spruit, C. Tran, Pierre Yves Andrews, Necip Fazil Ayan, Shruti Bhosale, Sergey Edunov, Angela Fan, Cynthia Gao, Vedanuj Goswami, Francisco (Paco) Guzmán, Philipp Koehn, Alexandre Mourachko, Christophe Ropers, Safiyyah Saleem, Holger Schwenk, and Jeff Wang. No language left behind: Scaling human-centered machine translation. *ArXiv*, abs/2207.04672, 2022. https://arxiv.org/abs/2207.04672.

Qwen Team. Qwen3 technical report, 2025. https://arxiv.org/abs/2505.09388.

Aaron van den Oord, Oriol Vinyals, and Koray Kavukcuoglu. Neural discrete representation learning. In *Proceedings of the 31st International Conference on Neural Information Processing Systems*, NIPS'17, page 6309–6318, Red Hook, NY, USA, 2017. Curran Associates Inc. ISBN 9781510860964.

Ashish Vaswani, Noam Shazeer, Niki Parmar, Jakob Uszkoreit, Llion Jones, Aidan N. Gomez, Lukasz Kaiser, and Illia Polosukhin. Attention is all you need. In *Advances in Neural Information Processing Systems*, volume 30. Curran Associates, Inc., 2017. https://papers.nips.cc/paper/7181-attention-is-all-you-need.

Mathurin Videau, Badr Youbi Idrissi, Alessandro Leite, Marc Schoenauer, Olivier Teytaud, and David Lopez-Paz. From bytes to ideas: Language modeling with autoregressive u-nets. *arXiv preprint arXiv:2506.14761*, 2025.

Junxiong Wang, Tushaar Gangavarapu, Jing Nathan Yan, and Alexander M. Rush. Mambabyte: Token-free selective state space model, 2024. https://arxiv.org/abs/2401.13660.

Linting Xue, Aditya Barua, Noah Constant, Rami Al-Rfou, Sharan Narang, Mihir Kale, Adam Roberts, and Colin Raffel. ByT5: Towards a token-free future with pre-trained byte-to-byte models. *Transactions of the Association for Computational Linguistics*, 10:291–306, 2022. doi: 10.1162/tacl_a_00461. https://aclanthology.org/2022.tacl-1.17/.

Jian Yang, Shawn Guo, Lin Jing, Wei Zhang, Aishan Liu, Chuan Hao, Zhoujun Li, Wayne Xin Zhao, Xianglong Liu, Weifeng Lv, and Bryan Dai. Scaling laws for code: Every programming language matters, 2025. https://arxiv.org/abs/2512.13472.

Qihang Yu, Mark Weber, Xueqing Deng, Xiaohui Shen, Daniel Cremers, and Liang-Chieh Chen. An image is worth 32 tokens for reconstruction and generation. In *The Thirty-eighth Annual Conference on Neural Information Processing Systems*, 2024. https://openreview.net/forum?id=tOXoQPRzPL.

Rowan Zellers, Ari Holtzman, Yonatan Bisk, Ali Farhadi, and Yejin Choi. Hellaswag: Can a machine really finish your sentence? In *Proceedings of the 57th Annual Meeting of the Association for Computational Linguistics*, 2019.

Ciyou Zhu, Richard H Byrd, Peihuang Lu, and Jorge Nocedal. Algorithm 778: L-bfgs-b: Fortran subroutines for large-scale bound-constrained optimization. *ACM Transactions on Mathematical Software (TOMS)*, 23(4):550–560, 1997.

Appendix

A Model Scaling: Technical Details

In this section, we describe the model architectures in detail.

The core experiments were conducted with BLT models (Pagnoni et al., 2025). We followed the original implementation with a few notable exceptions. As noted in Section 2, we find that the local modules should be wide (high number of heads) and shallow (low number of layers). To achieve such a shape, we set the number of layers in each local module to the ceiling of one-fourth of the number of global layers, and the local head count to the ceiling of one-fourth of the number of global heads, plus 8. The cross-attention key-query duplication factor k is set to the ceiling of one-eighth of the global module's head count. The hidden dimension of the local modules is set to 64 times the number of heads. This scaling recipe ensures that the compute overhead introduced by the local modules is comparable to the embedding layers found in isotropic models of similar scale.

An important divergence from the original BLT architecture of Pagnoni et al. (2025) is the omission of hash embeddings. To compensate for the reduced capacity for encoding the input, we increase the number of layers in the encoder to match the decoder (originally, the encoder has only one layer). Table 4 presents the scales and architecture hyperparameters of all BLT models used in this work.

Similarly, Table 5 outlines the scaling recipe for subword tokenized models.

We compare the compute spend in the latent module as a percentage of the total inference compute for both families of models in Table 6. We observe that with our scaling recipes, the global module takes up a similar share of compute in the BLT architecture as in the isotropic model when the model scale and compression rate are matched. We observe that decreasing compression rate or increasing model size correlates with a higher relative utilization of the global model.

B Scaling Laws: Technical Details

We characterize compute-optimal scaling through a two-stage fitting procedure.

B.1 Scaling Law I

We fit the scaling laws to find optimal data and parameters as described in Equations 1 and 3. As noted in the methodology, we restrict this fit to the parameters of the global latent model (excluding encoder/decoder and embeddings) to ensure consistency across tokenization methods.

We perform the fit using the L-BFGS-B (Zhu et al., 1997) algorithm with a gradient tolerance of 10^{-10}. To ensure robust convergence, we employ a grid search for initialization:

1. We first compute an Ordinary Least Squares (OLS) solution $(\alpha_{\text{OLS}}, \beta_{\text{OLS}}, B_{\text{OLS}}, N_{\text{OLS}})$ on the log-transformed data to serve as a prior.
2. We define a search grid by perturbing the OLS solution. We test 13 values for each parameter, resulting in 13^4 total initialization points (though we fix α and β ranges tighter than B_0 and N_0).

The grid is constructed as follows:

- $\log(B_{\text{init}}) \in \{\log(B_{\text{OLS}}) + \epsilon : \epsilon \in [-3, 3]\}$
- $\log(N_{\text{init}}) \in \{\log(N_{\text{OLS}}) + \epsilon : \epsilon \in [-3, 3]\}$
  - $\alpha_{\text{init}} \in \{\alpha_{\text{OLS}} + \epsilon : \epsilon \in [-0.3, 0.3]\}$
  - $\beta_{\text{init}} \in \{\beta_{\text{OLS}} + \epsilon : \epsilon \in [-0.3, 0.3]\}$

We select the solution that minimizes the sum of squares loss objective. The BFGS algorithm obtained the parameter values similar to OLS regardless of its starting point.

Global (Latent Module)				Local (Encoder/Decoder)				Cross-Attention		Total
Layers	Heads	Dim	Params	Layers	Heads	Dim	Params	Heads	k	Params
5	5	640	25M	2	10	640	10M	10	1	50M
6	6	768	43M	2	10	640	10M	10	1	68M
7	7	896	67M	2	10	640	10M	10	1	93M
8	8	1024	101M	2	10	640	10M	10	1	127M
9	9	1152	143M	3	12	768	21M	12	2	199M
10	10	1280	197M	3	12	768	21M	12	2	253M
11	11	1408	262M	3	12	768	21M	12	2	318M
12	12	1536	340M	3	12	768	21M	12	2	396M
13	13	1664	432M	4	12	768	28M	12	2	506M
14	14	1792	540M	4	12	768	28M	12	2	613M
15	15	1920	664M	4	12	768	28M	12	2	738M
16	16	2048	805M	4	12	768	28M	12	2	880M
17	17	2176	966M	5	14	896	48M	14	3	1.1B
18	18	2304	1.1B	5	14	896	48M	14	3	1.3B
19	19	2432	1.3B	5	14	896	48M	14	3	1.5B
20	20	2560	1.6B	5	14	896	48M	14	3	1.7B
21	21	2688	1.8B	6	14	896	58M	14	3	2.0B
22	22	2816	2.1B	6	14	896	58M	14	3	2.2B
23	23	2944	2.4B	6	14	896	58M	14	3	2.5B
24	24	3072	2.7B	6	14	896	58M	14	3	2.9B
25	25	3200	3.1B	7	16	1024	88M	16	4	3.3B
26	26	3328	3.5B	7	16	1024	88M	16	4	3.7B
27	27	3456	3.9B	7	16	1024	88M	16	4	4.1B
28	28	3584	4.3B	7	16	1024	88M	16	4	4.6B
29	29	3712	4.8B	8	16	1024	101M	16	4	5.1B
30	30	3840	5.3B	8	16	1024	101M	16	4	5.6B
31	31	3968	5.9B	8	16	1024	101M	16	4	6.1B
32	32	4096	6.4B	8	16	1024	101M	16	4	6.7B

Table 4 The configuration of latent tokenized models (BLT architecture) used in scaling experiments.

Global (Latent Module)				Local Parameters (Embeddings)			Total Parameters		
Layers	Heads	Dim	Params	Char	BPE	SuperBPE	Char	BPE	SuperBPE
5	5	640	25M	96M	82M	128M	121M	107M	153M
6	6	768	43M	115M	98M	154M	158M	141M	196M
7	7	896	67M	134M	115M	179M	202M	182M	247M
8	8	1024	101M	154M	131M	205M	254M	232M	306M
9	9	1152	143M	173M	148M	230M	316M	291M	374M
10	10	1280	197M	192M	164M	256M	389M	360M	453M
11	11	1408	262M	211M	180M	282M	473M	442M	543M
12	12	1536	340M	230M	197M	307M	570M	536M	647M
13	13	1664	432M	250M	213M	333M	682M	645M	765M
14	14	1792	540M	269M	229M	358M	808M	769M	898M
15	15	1920	664M	288M	246M	384M	952M	909M	1.0B
16	16	2048	805M	307M	262M	410M	1.1B	1.1B	1.2B
17	17	2176	966M	326M	279M	435M	1.3B	1.2B	1.4B
18	18	2304	1.1B	346M	295M	461M	1.5B	1.4B	1.6B
19	19	2432	1.3B	365M	311M	486M	1.7B	1.7B	1.8B
20	20	2560	1.6B	384M	328M	512M	2.0B	1.9B	2.1B
21	21	2688	1.8B	403M	344M	538M	2.2B	2.2B	2.4B
22	22	2816	2.1B	422M	360M	563M	2.5B	2.5B	2.7B
23	23	2944	2.4B	442M	377M	589M	2.8B	2.8B	3.0B
24	24	3072	2.7B	461M	393M	614M	3.2B	3.1B	3.3B
25	25	3200	3.1B	480M	410M	640M	3.6B	3.5B	3.7B
26	26	3328	3.5B	499M	426M	666M	4.0B	3.9B	4.1B
27	27	3456	3.9B	518M	442M	691M	4.4B	4.3B	4.6B
28	28	3584	4.3B	538M	459M	717M	4.9B	4.8B	5.0B
29	29	3712	4.8B	557M	475M	742M	5.4B	5.3B	5.5B
30	30	3840	5.3B	576M	492M	768M	5.9B	5.8B	6.1B
31	31	3968	5.9B	595M	508M	794M	6.5B	6.4B	6.7B
32	32	4096	6.4B	614M	524M	819M	7.1B	7.0B	7.3B

Table 5 The configuration of subword tokenized models (isotropic). Parameter differences across tokenizers arise from varying vocabulary sizes V. For Character: $V = 148,000$, for BPE: $V = 128,000$, for SuperBPE $V = 200,000$.

	Latent Tokenization						Subword Tokenizetion		
Scale	T=1	T=2	T=4	T=6	T=8	T=12	T=1.01	T=4.57	T=6.16
5	66%	43%	24%	17%	13%	9%	34%	27%	18%
6	75%	55%	35%	25%	20%	14%	41%	34%	24%
7	82%	65%	45%	35%	28%	20%	47%	41%	30%
8	87%	73%	55%	44%	36%	27%	52%	47%	35%
9	79%	63%	44%	34%	27%	20%	57%	52%	41%
10	84%	70%	52%	41%	34%	25%	61%	57%	45%
11	87%	75%	58%	48%	41%	31%	65%	62%	50%
12	89%	79%	64%	54%	47%	37%	68%	65%	54%
13	89%	78%	63%	53%	46%	36%	71%	69%	58%
14	91%	82%	68%	58%	51%	41%	73%	72%	62%
15	92%	84%	72%	63%	56%	46%	76%	74%	65%
16	93%	87%	76%	68%	61%	51%	78%	77%	67%
17	90%	82%	69%	59%	52%	42%	80%	79%	70%
18	91%	84%	72%	63%	57%	46%	81%	81%	72%
19	93%	86%	75%	67%	60%	50%	83%	82%	74%
20	93%	88%	78%	70%	64%	54%	84%	84%	76%
21	93%	87%	77%	70%	63%	53%	85%	85%	78%
22	94%	89%	80%	72%	66%	57%	86%	86%	79%
23	95%	90%	82%	75%	69%	60%	87%	87%	81%
24	95%	91%	84%	77%	72%	63%	88%	88%	82%
25	93%	88%	79%	71%	65%	56%	89%	89%	83%
26	94%	89%	81%	74%	68%	59%	89%	89%	84%
27	95%	90%	82%	76%	70%	61%	90%	90%	85%
28	95%	91%	84%	78%	73%	64%	91%	91%	86%
29	95%	91%	83%	77%	72%	63%	91%	91%	87%
30	95%	92%	85%	79%	74%	66%	92%	92%	88%
31	96%	92%	86%	81%	76%	68%	92%	92%	88%
32	96%	93%	87%	82%	78%	70%	92%	93%	89%

Table 6 The compute cost per byte by global model as percentage of compute cost per byte of the whole model. The first column (Scale) denotes number of layers and heads of global module. In latent tokenization compression rate $T \in \{1, 2, 4, 6, 8, 12\}$ is set as hyperparameter, whereas in subword tokenization it is determined by the tokenizer (Character $T = 1.01$, BPE $T = 4.57$, SuperBPE $T = 6.16$)

B.2 Scaling Law II

In the second stage, we fit the power law for optimal loss $L^\star(C,T) \simeq L_0 C^\gamma + f(T)$. Unlike Stage I, we use the total compute budget, for this fit, including the cost of the encoder, decoder, and embeddings.

We fit the parameters L_0, γ, and the compression-specific offsets $f(T)$ simultaneously. We again use BFGS with a grid search for initialization. The grid spans 13 values for L_0 and γ (169 combinations):

- $\log(L_{\text{init}}) \in [-3, 3]$
- $\gamma_{\text{init}} \in [-0.6, 0.0]$

The initial value for $f(T)$ is set to the mean loss observed at compression rate T. During optimization, we bound the parameters to physically plausible ranges: $\log(L_0) \in [-30, 30]$, $\gamma \in [-2, 0]$, and $f(T) \in [-5, 5]$.

B.3 Derivation and Validation of Scaling Law II

Residual model	E	F	T_0	δ	RMSE	R^2	$\bar{R}^2$
Mean of residuals (Eq. 8)	0.7075	—	—	—	0.0260	0.903	0.896
Constant $T^\star$ (Eq. 9)	0.7075	0.0341	3.73	—	0.0115	0.996	0.995
Compute-dependent $T^\star$ (Eq. 7)	0.7075	0.0341	14.9	0.0302	**0.0086**	**0.997**	**0.996**

Table 7 Comparison of the three considered forms for modeling $f(C,T)$ residuals in Equation 6. All functions were fitted using the 48 runs with compute budgets less than or equal to 1×10^{21} FLOPs. To test extrapolation accuracy, Root Mean Square Error was computed for models trained at 2×10^{21} FLOPs across 8 different compression rates. All evaluations of extrapolation performance and goodness-of-fit (standard and adjusted for the number of variables) indicate that the model with compute-dependent compression rate offers the best fit and extrapolation accuracy in loss estimation.

As described in Section 3.3, we begin the search for the scaling law equation by assuming the classical form from Kaplan et al. (2020), disregarding the role of compression. It is presented by Equation 6:

$$L^\star(C,T) \simeq L_0 \times C^\gamma + f(C,T)$$

First, we fit the first part of the scaling law, and then we examine the functions that would give the best approximation of $f(C,T)$ (residuals of the fit) with minimal complexity. We consider the following candidates for $f(C,T)$:

Mean of the residuals is equivalent to the "irreducible loss" term or intercept used in many scaling fits. It is the simplest form of $f(C,T)$, yet it still completely disregards the role of compression on loss. We consider the following form of irreducible loss:

$$f(C,T) = E \tag{8}$$

Constant optimal compression ($T^\star$) is an assumption that the loss is always minimal for one compression rate, regardless of compute budget C. By an inspection of $f(C,T)$ residuals in Figure 6, we observe that they are distributed along a non-monotonic convex function of T, with a minimum at some point T_0. We assume that a quadratic function fits this relation well. Considering that T is on a logarithmic scale, we propose the following equation for residuals (including also irreducible loss):

$$f(C,T) = F \times (\log(T) - \log(T_0))^2 + E = F \times \log^2\left(\frac{T}{T_0}\right) + E \tag{9}$$

Compute-dependent optimal compression ($T^\star$) is based on a hypothesis that the optimal compression depends on compute budget. We observe that the minimum of the quadratic function modeling $f(T,C)$ described in the last paragraph shifts to a lower value with an increase of the training budget. To account for that, we

include the effect of the compute budget in the log-quadratic function, arriving at the following formulation of Equation 7:

$$f(C,T) = F \times \log^2\left(\frac{C^{\delta}T}{T_0}\right) + E$$

To validate the extrapolation accuracy of the three candidate formulas, we fitted scaling laws for results of models trained for 8 computation budgets from 5×10^{18} to 1×10^{21}, and 6 compression rates. For each compression rate and budget, we use the optimal model size (and training data) estimated by the Scaling Law I. Then we validate the obtained scaling laws by comparing expected vs. obtained loss for models trained with a higher compute budget: 2×10^{21}. In Table 7, we observe that the last formulation, making an assumption that the optimal compression rate is compute-dependent, obtains significantly lower mean square error in extrapolation than other candidate formulations. Moreover, the fit using this formula obtains the highest goodness-of-fit coefficient, both standard (R^2) and adjusted for the number of fitted variables ($\bar{R}^2$). Therefore, we decided to choose this formulation for the final version of the scaling law.

B.4 Loss Sensitivity to Compression Rate

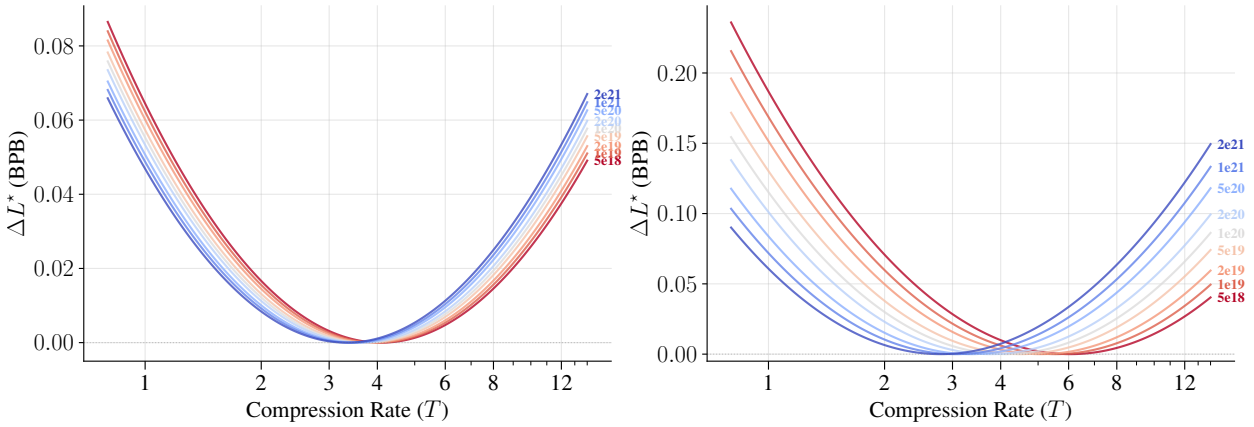

(a) Latent Tokenization **(b)** Subword Tokenization

Figure 16 The BPB deterioration across compression compared to the value at optimal compression rate. $\Delta L^\star$ function was predicted based on Scaling Law II fit.

Figure 16 shows marginal sensitivity of loss to the choice of compression rate. We observe that compression rate close to optimal has minimal impact on loss, yet diverging further from the optimum can cause up to 0.2 and 0.1 deterioration in test BPB for subword and latent tokenized models respectively.

B.5 Confidence Intervals

We compute 95% confidence intervals for the fitted parameters $\hat{\boldsymbol{\theta}} \in \mathbb{R}^p$ from n data points, where p is the number of parameters. $\mathcal{L}(\boldsymbol{\theta})$ denotes the sum of squares loss evaluated at $\boldsymbol{\theta}$, and $\mathbf{e}_k$ be the k-th standard basis vector in $\mathbb{R}^p$.

The Hessian $H \in \mathbb{R}^{p \times p}$ of $\mathcal{L}$ is estimated via central finite differences with step size $\epsilon = 10^{-5}$:

$$H_{ij} = \frac{\mathcal{L}_{ij}^{++} - \mathcal{L}_{ij}^{+-} - \mathcal{L}_{ij}^{-+} + \mathcal{L}_{ij}^{--}}{4\,\epsilon^2} \tag{10}$$

where

$$\mathcal{L}_{ij}^{s_1 s_2} = \mathcal{L}\big(\boldsymbol{\theta} + s_1\,\epsilon\,\mathbf{e}_i + s_2\,\epsilon\,\mathbf{e}_j\big) \qquad s_1, s_2 \in \{+,-\} \tag{11}$$

The residual variance is estimated as

$$\hat{\sigma}^2 = \frac{\sum_{i=1}^{n} r_i^2}{n-p} \tag{12}$$

where $r_i = y_i - \hat{y}_i$ is the i-th residual (observed minus predicted value). The parameter covariance matrix is

$$\hat{\Sigma} = \hat{\sigma}^2 \, H^{-1} \tag{13}$$

The 95% confidence interval for each parameter $\hat{\boldsymbol{\theta}}_k$ is:

$$\hat{\boldsymbol{\theta}}_k \pm t \cdot \sqrt{\hat{\Sigma}_{kk}} \tag{14}$$

where $\sqrt{\hat{\Sigma}_{kk}}$ is the standard error for estimation of $\hat{\boldsymbol{\theta}}_k$ and t is the two-sided 95% critical value of Student's t-distribution with $n - p$ degrees of freedom.

C Impact of Tokenization Method

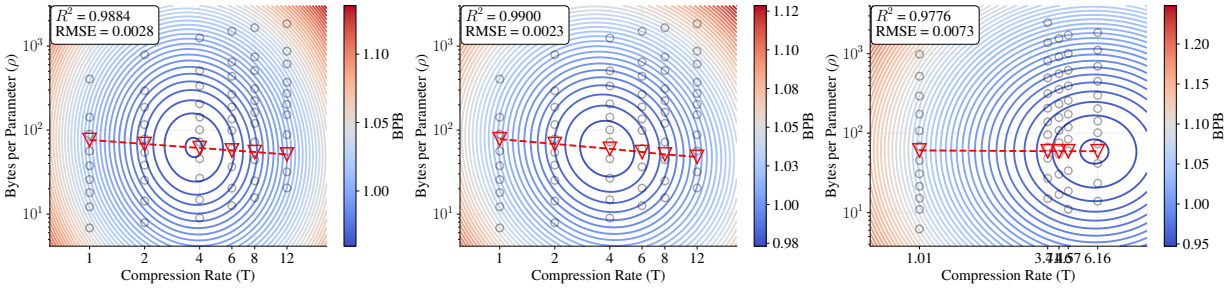

(a) Latent Tokenization (Entropy) **(b)** Latent Tokenization (Fixed Size) **(c)** Subword Tokenization

Figure 17 Comparison of three-dimensional IsoFLOPs ($C = 10^{20}$) for three methods of tokenization: Latent Entropy, Latent Fixed Size (each latent token has fixed size of T bytes), and Subword. The loss profile is visibly similar across the methods, with optimal loss achieved along constant bytes per parameter.

Tokenization Method	$\rho^\star$	$T^\star$	BPB
Latent (Entropy)	62.1	3.71	0.960
Latent (Fixed)	60.0	3.87	0.973
Subword	58.8	5.36	0.947

Table 8 Compute-optimal bytes per parameter ($\rho^\star$) and compression rate ($T^\star$) for different methods. The values are close to each other, except for subword $T^\star$.

We compare our results for different methods of tokenization: latent (with entropy supervision) and subword, as described in the main text. Moreover, we compare the results with another method of latent tokenization, where all latent tokens are of the same fixed size in bytes equal to compression rate. In Figure 17, we see similar loss profiles across different methods. For all the methods and compression rates, the optimal configurations fall at ≈ 60 bytes per parameter ratio (ρ). In Table 8, we further observe that for two latent tokenization methods the optimal compression rate is similar, while in subword tokenization it is higher. This is due to an imperfect IsoFLOP paraboloid fit caused by poor performance of character-level models ($T = 1.01$) under the considered budget, skewing optimal T to be higher than in reality. Based on the more reliable Scaling Law II estimation (see Section 4) we expect to observe lower optimal compression rate for this budget: $T^\star = 4.11$. For comparison, optimal compression rate for latent models based on Scaling Law is $T^\star = 3.67$.

D Impact of Mixing Languages

Language	Parity	$\rho_l^\star$		$T_l^\star$		BPB
		Value	Ratio	Value	Ratio	
English	1.0	71.8	1.00	3.38	1.00	1.101
French	1.2	72.5	1.01	3.65	1.08	0.931
Vietnamese	1.4	70.3	0.98	4.12	1.22	0.720
Arabic	1.6	76.5	1.07	3.84	1.14	0.667
Russian	2.0	77.6	1.08	5.03	1.49	0.532
Hindi	2.6	68.9	0.96	6.32	1.87	0.387

Table 9 Compute-optimal bytes per parameter ($\rho_l^\star$), compression rate ($T_l^\star$) compared to cross-lingual parity. Results for multilingual models, trained jointly on all six languages with $C = 10^{20}$ FLOPs budget. The parity and compute-optimal ratios are proportions between each language and English baseline.

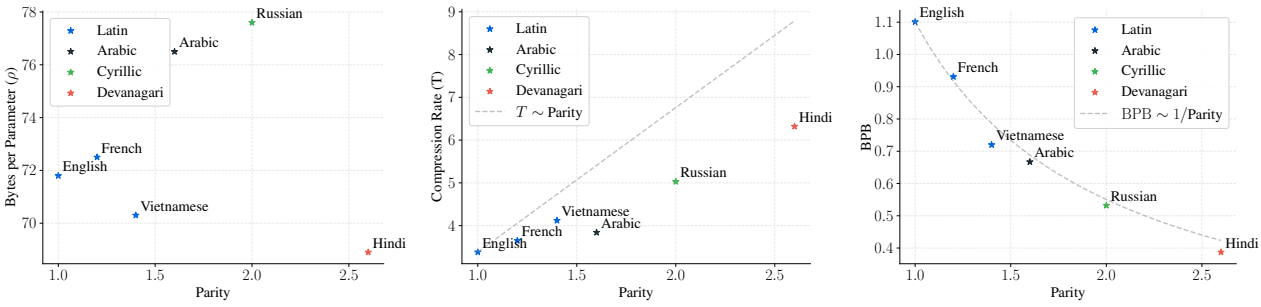

(a) bytes per parameter **(b)** compression rate **(c)** BPB

Figure 18 The optimal bytes per parameter, compression rate, and BPB for multilingual models trained on all languages jointly for $C = 10^{20}$ FLOPs. The optimal values are compared against parity on x-axis.

To examine the impact of mixing languages during training, we train a set of models jointly on multilingual data in six languages (including English), described in Section 5. To enforce an equitable training signal across languages, we sample languages with weights equal to their parity. For instance, we train on 2.6 more bytes in Hindi than in English, but we expect the two samples to be matched in information value. All training runs are constrained to a fixed budget of $C = 10^{20}$ FLOPs; thus, multilingual models see less in-language data per language than their monolingual counterparts.

The optimal values of bytes per parameter and compression rate for each language are computed based on fits to the in-language test set, the results are gathered in Table 9. Figure 18a shows that the optimal bytes per parameter is similar across languages. This contrasts with the findings in Section 5, where the optimal bytes per parameter was language-dependent and correlated with parity. Notably, the multilingual optimal bytes per parameter ($\rho^\star \approx 70$) is close to the median of the language-specific optimal values, $\rho_l^\star$. As in the monolingual experiments, we observe that the optimal compression rate (Figure 18b) is correlated with parity. The multilingual optimal values are lower than the corresponding monolingual ones. Test BPB (Figure 18c) is inversely correlated with parity, in line with the results of Section 5. As expected, multilingual models perform worse than monolingual ones due to the smaller amount of in-language data.

E Comparison with "Scaling Laws with Vocabulary"

Tao et al. (2024) posited similar research questions to ours regarding the role of tokenization in scaling laws, yet reached significantly different conclusions, showing that vocabularies (and thus compression rate) should increase with model scale. Meanwhile, we observe that the compute optimal compression rate does not increase with model scale. We identify the following methodological differences that explain discrepancies:

Approach to embedding-layer compute and vocabulary size The main difference is how compression is connected to the size of the embedding layers. Tao et al. (2024) control compression rate by changing the vocabulary size, which affects the size of the embedding layer. This leads to a preference for smaller vocabularies at low compute and parameter budgets, so the FLOPs saved in embedding layers can be used for significantly longer training. In our experiments, vocabulary cost is (almost) the same regardless of compression, thanks to the use of BLT (Pagnoni et al., 2025) or alternative subword methods such as SuperBPE (Liu et al., 2025). Therefore, our results extrapolate better to larger scales, where the cost of the embedding layer is negligible, as seen in Table 6.

Considered compression range BPE achieves a narrow compression rate range (by our estimates, $T \in [3, 4.5]$ bytes per token). Considering only compressions attainable by BPE allows us to observe only a portion of the loss profile, one that falls below the optimal compression value.

Evaluation Both works use normalized negative log likelihood enabling a fair comparison across tokenizers. Tao et al. (2024) match validation context length in tokens, so the number of bytes in an evaluation example varies with vocabulary. We match the number of bytes across compression levels (e.g., if with compression rate $T = 4$ we evaluate on 2048 tokens per example, then with compression rate $T = 8$ we evaluate on 1024 tokens). Because early bytes are harder than later bytes, matching validation context in tokens can favor higher-compression tokenizers (more "late" bytes in an example). This could explain why we do not see the same preference for high compression (large vocabulary) at larger scales. For further reference, SuperBPE (Liu et al., 2025) also matched evaluation context in bytes. Similarly to our results, they observed worse BPB scores for highly compressed SuperBPE compared to regular BPE.

F Supplementary Results

F.1 IsoFLOP Analysis across Compute Budgets

We present the IsoFLOPs across multiple compute budgets and compression rates for latent tokenized models in Figures 19. And for subword tokenized models in Figures 21. We observe that the optimal byte-per-parameter ratio $\rho^\star$ remains constant for most of the considered configurations, this trend is more visible for $C > 10^{20}$, where the compute of the global module becomes dominant, thus it is expected to hold also at larger scales.

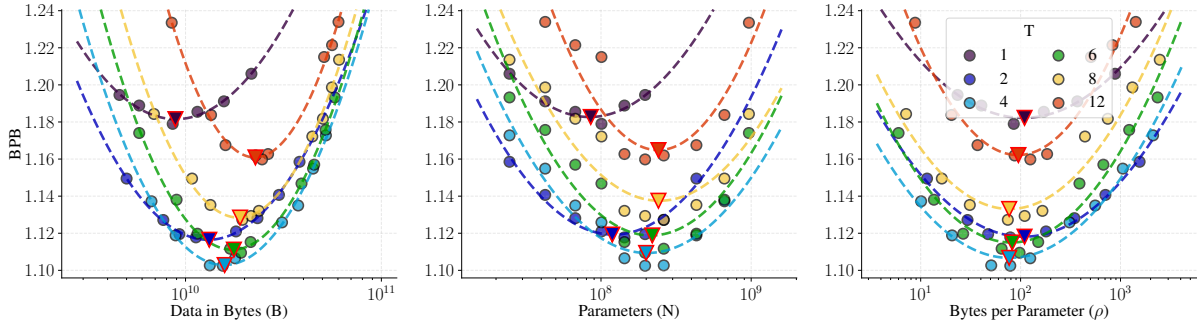

(a) $C = 10^{19}$ Latent Tokenization

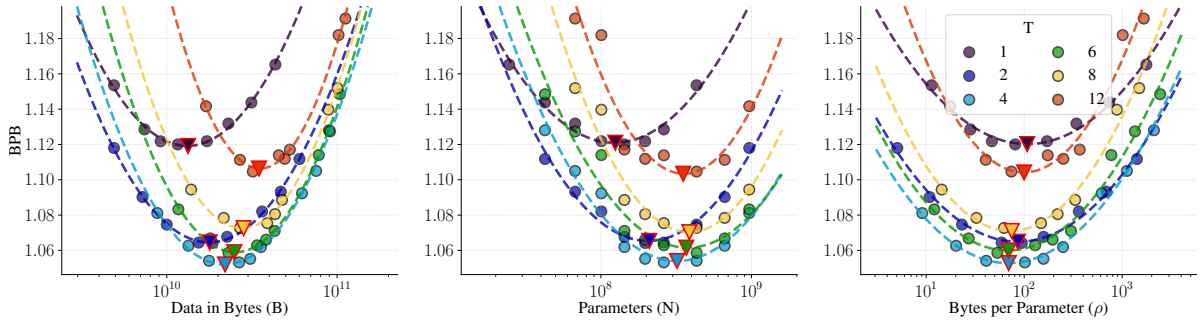

(b) $C = 2 \times 10^{19}$ Latent Tokenization

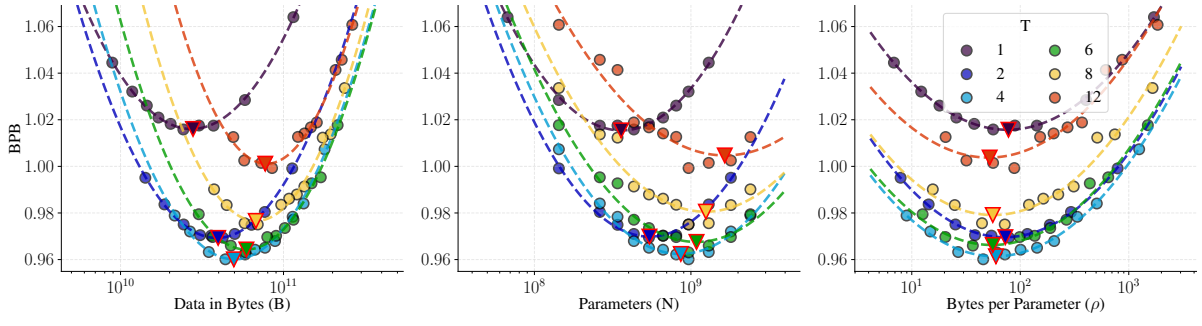

(c) $C = 10^{20}$ Latent Tokenization

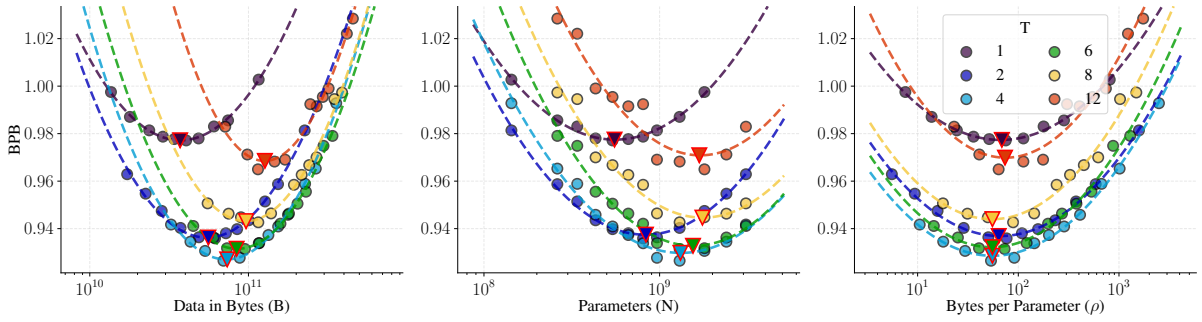

(d) $C = 2 \times 10^{20}$ Latent Tokenization

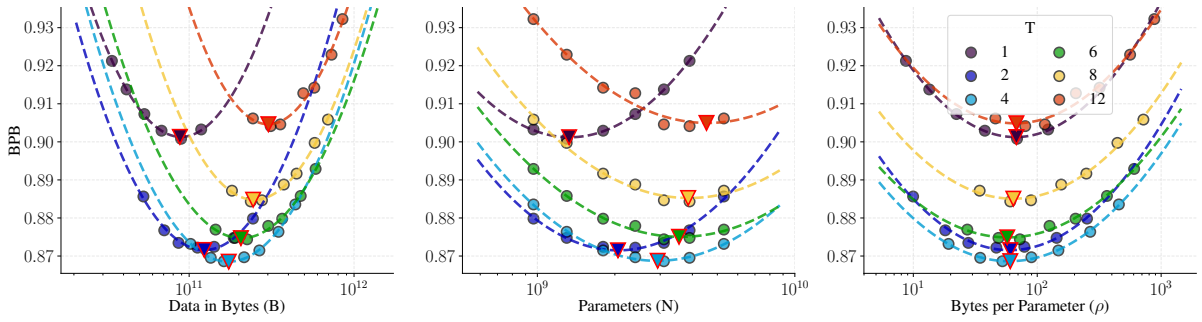

(e) $C = 10^{21}$ Latent Tokenization

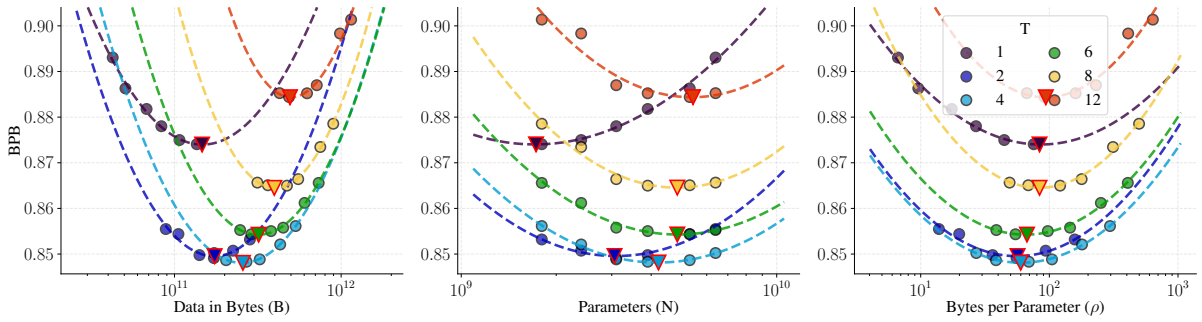

(f) $C = 2 \times 10^{21}$ Latent Tokenization

Figure 19 2-dimensional IsoFLOPs for latent tokenized models, as a function of data (B), parameters (N), or bytes per parameter ratio (ρ). Training budgets are indicated in each panel's caption. IsoFLOPs (parabolas) are fitted for each compression line to interpolate values of the loss.

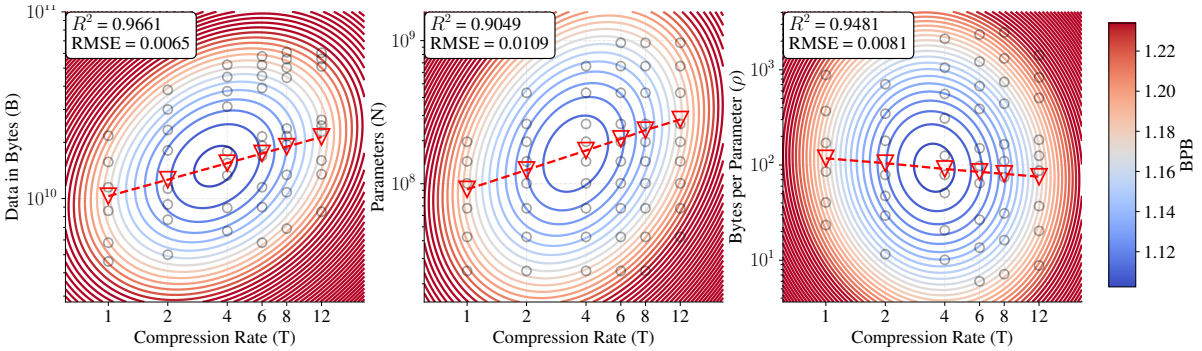

(a) $C = 10^{19}$ Latent Tokenization

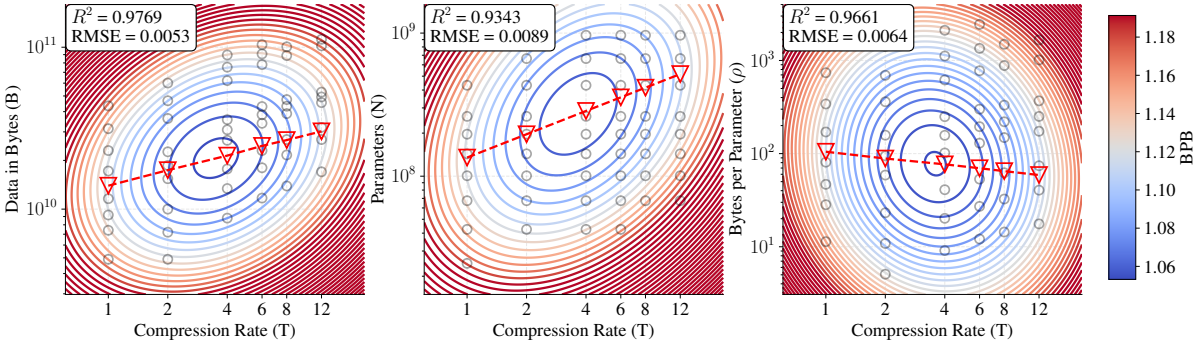

(b) $C = 2 \times 10^{19}$ Latent Tokenization

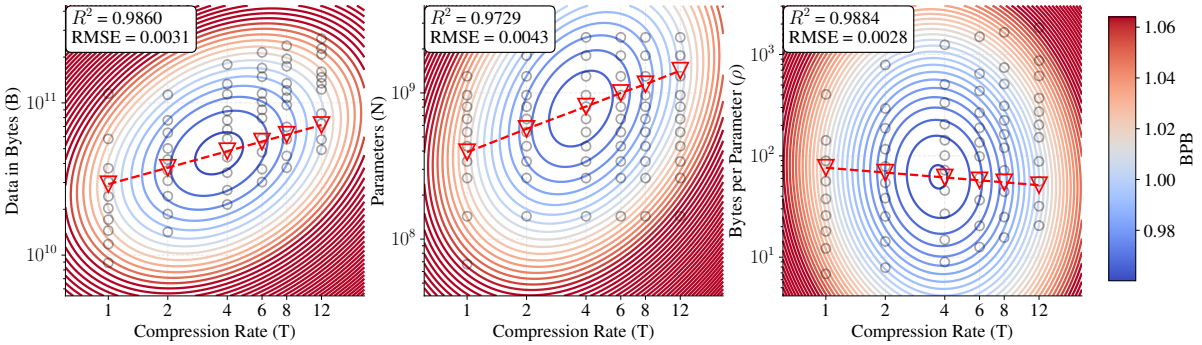

(c) $C = 10^{20}$ Latent Tokenization

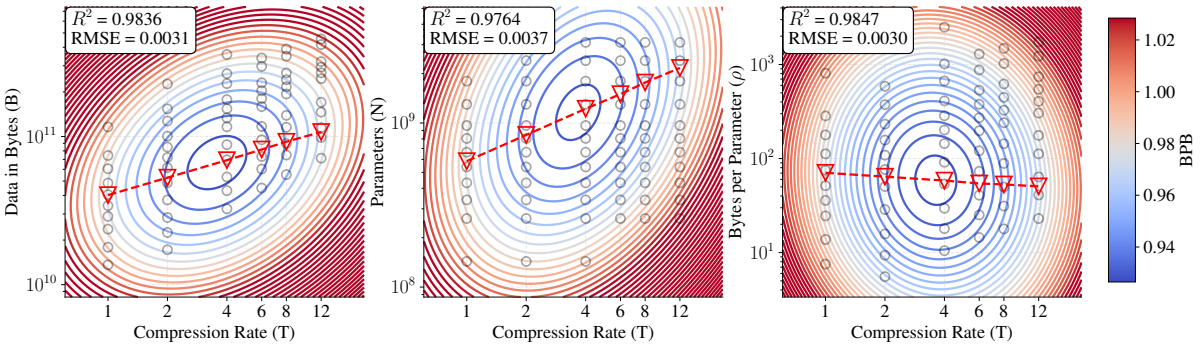

(d) $C = 2 \times 10^{20}$ Latent Tokenization

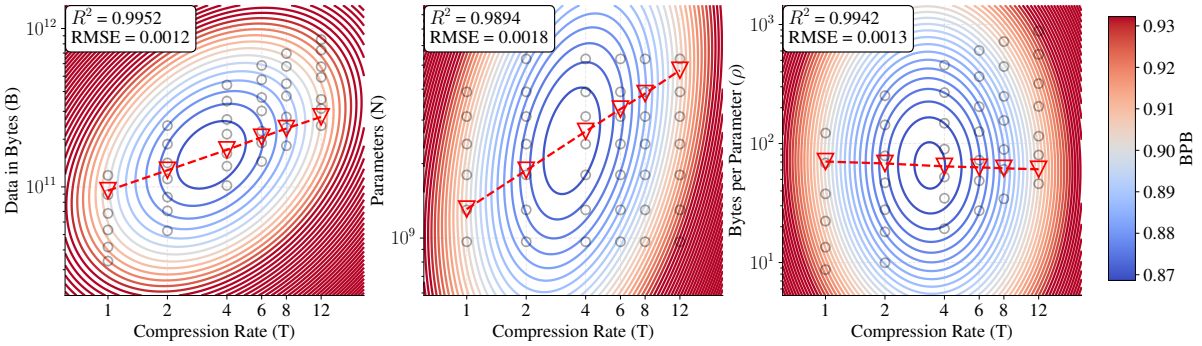

(e) $C = 10^{21}$ Latent Tokenization

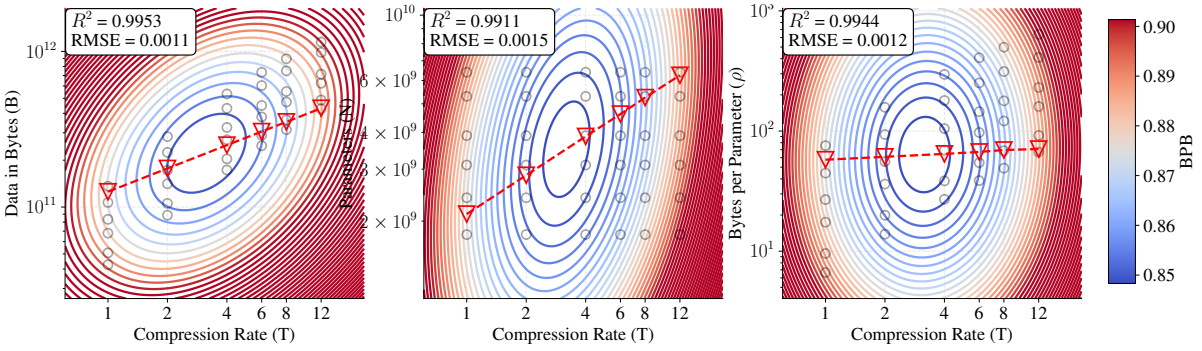

(f) $C = 2 \times 10^{21}$ Latent Tokenization

Figure 20 3-dimensional IsoFLOPs for latent tokenized models, as a function of compression rate and data (B), parameters (N), or bytes per parameter ratio (ρ). Training budgets are indicated in each figure's caption. IsoFLOPs (paraboloids) are jointly for all compression rates.

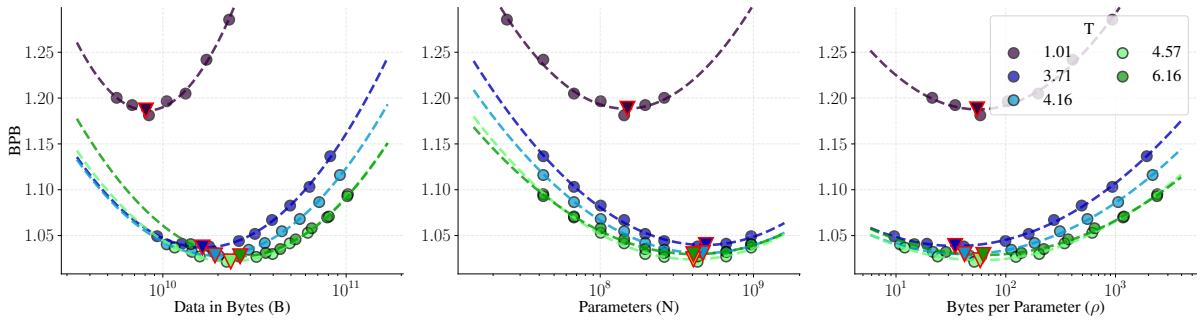

(a) $C = 5 \times 10^{19}$ Subword Tokenization

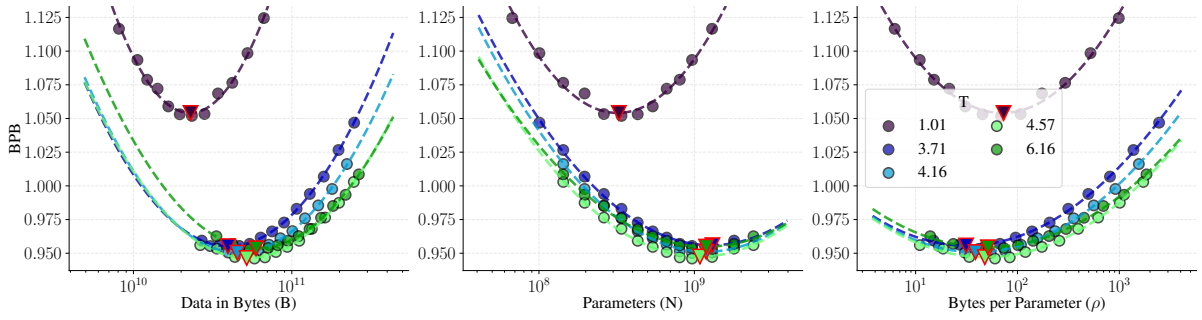

(b) $C = 10^{20}$ Subword Tokenization

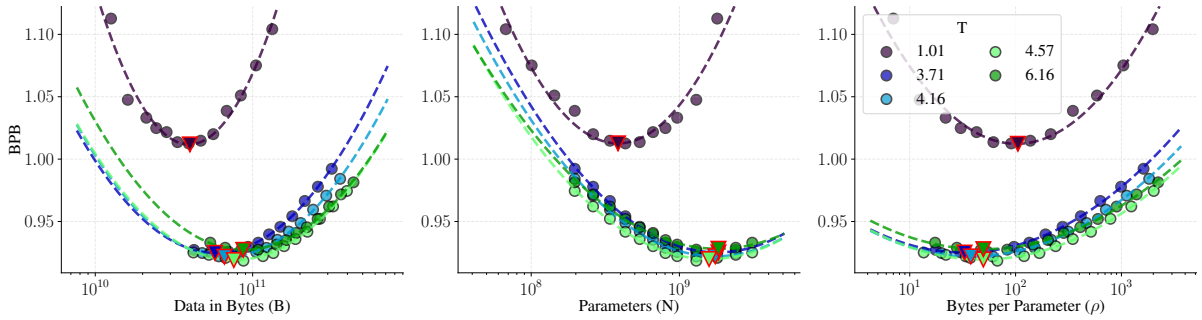

(c) $C = 2 \times 10^{20}$ Subword Tokenization

Figure 21 2-dimensional IsoFLOPs for subword tokenized models, as a function of data (B), parameters (N), or bytes per parameter ratio (ρ). Training budgets are indicated in each panel's caption. IsoFLOPs (parabolas) are fitted for each compression line to interpolate values of the loss.

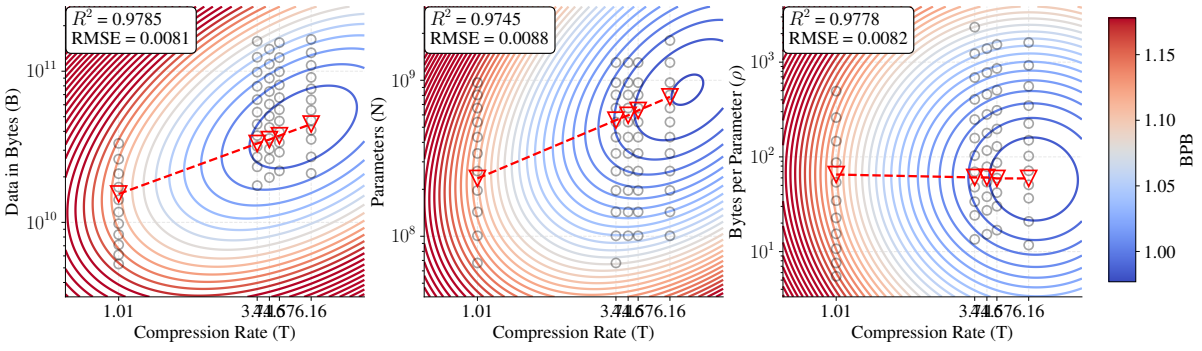

(a) $C = 5 \times 10^{19}$ Subword Tokenization

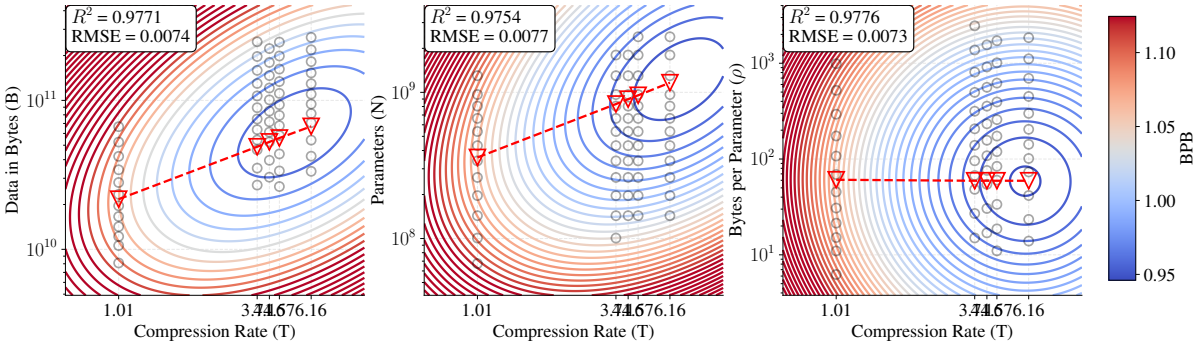

(b) $C = 10^{20}$ Subword Tokenization

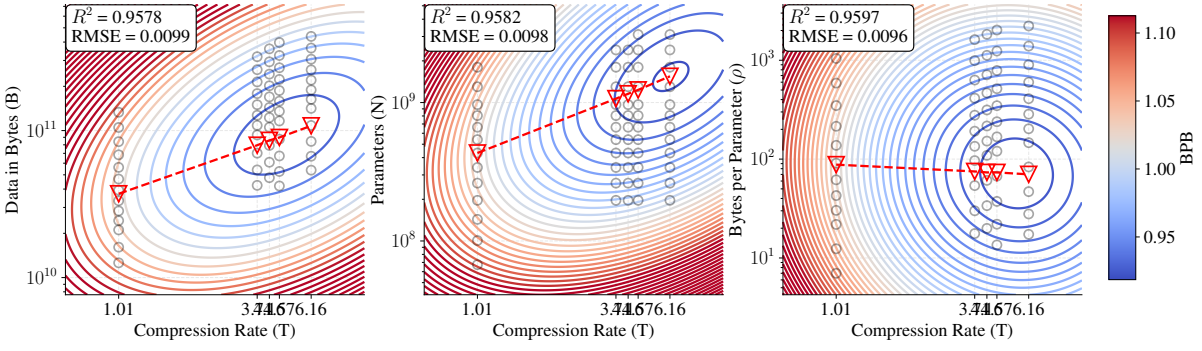

(c) $C = 2 \times 10^{20}$ Subword Tokenization

Figure 22 3-dimensional IsoFLOPs for subword tokenized models, as a function of compression rate and data (B), parameters (N), or bytes per parameter ratio (ρ). Training budgets are indicated in each figure's caption. IsoFLOPs (paraboloids) are jointly for all compression rates.

Compute	Latent Entropy					
(FLOPs)	1	2	4	6	8	12
1×10^{19}	1.1790	1.1178	**1.1025**	1.1095	1.1272	1.1598
2×10^{19}	1.1200	1.0642	**1.0532**	1.0587	1.0727	1.1047
5×10^{19}	1.0606	1.0080	**0.9987**	1.0049	1.0165	1.0422
1×10^{20}	1.0158	0.9694	**0.9601**	0.9631	0.9751	0.9993
2×10^{20}	0.9771	0.9359	**0.9265**	0.9314	0.9427	0.9650
5×10^{20}	0.9333	0.8974	**0.8933**	0.8990	0.9085	0.9278
1×10^{21}	0.9008	0.8722	**0.8686**	0.8744	0.8843	0.9041
2×10^{21}	0.8741	0.8491	**0.8483**	0.8543	0.8650	0.8844
Compression:	1	2	4	6	8	12

Table 10 Comparison of the lowest BPB obtained by latent tokenized models for specific compute budgets.

F.2 Optimal Data and Parameters across Compute Budgets

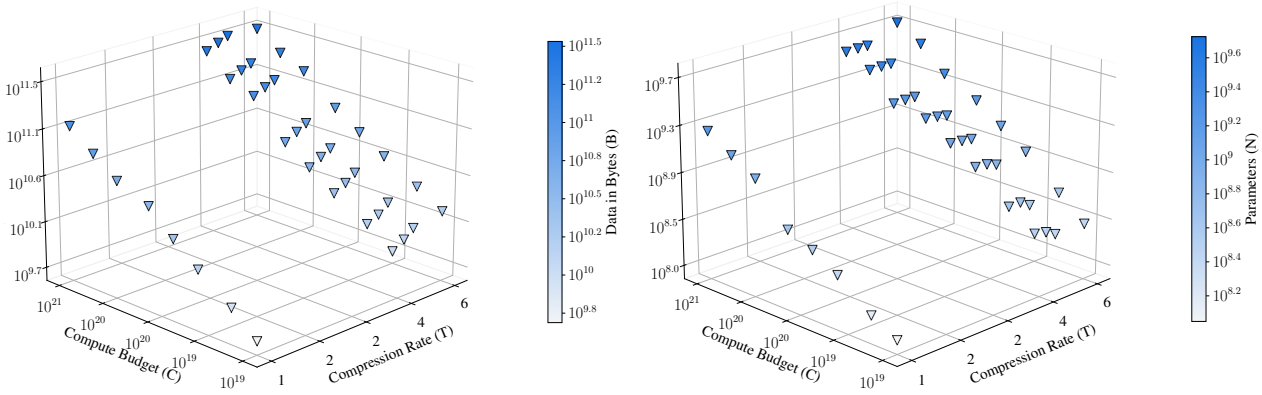

(a) Amount of data

(b) Model size

Figure 23 Optimal data and model size configurations for each compute budget and compression rate (subword tokenized models).

Figure 23 shows the optimal data in bytes B^* and parameter counts N^* across compressions and compute budgets for subword tokenized models.

F.3 Loss Obtained by Optimal Configurations

In Tables 10 and 2, we present the best scores obtained by models (i.e., not derived from scaling law) respectively for latent and subword tokenized models.

F.4 Multilingual 2D IsoFLOP

In Figure 24, we present 2-dimensional IsoFLOP for six considered languages. The visualization is based on the same data as used for 3-dimensional IsoFLOP in Figure 11.

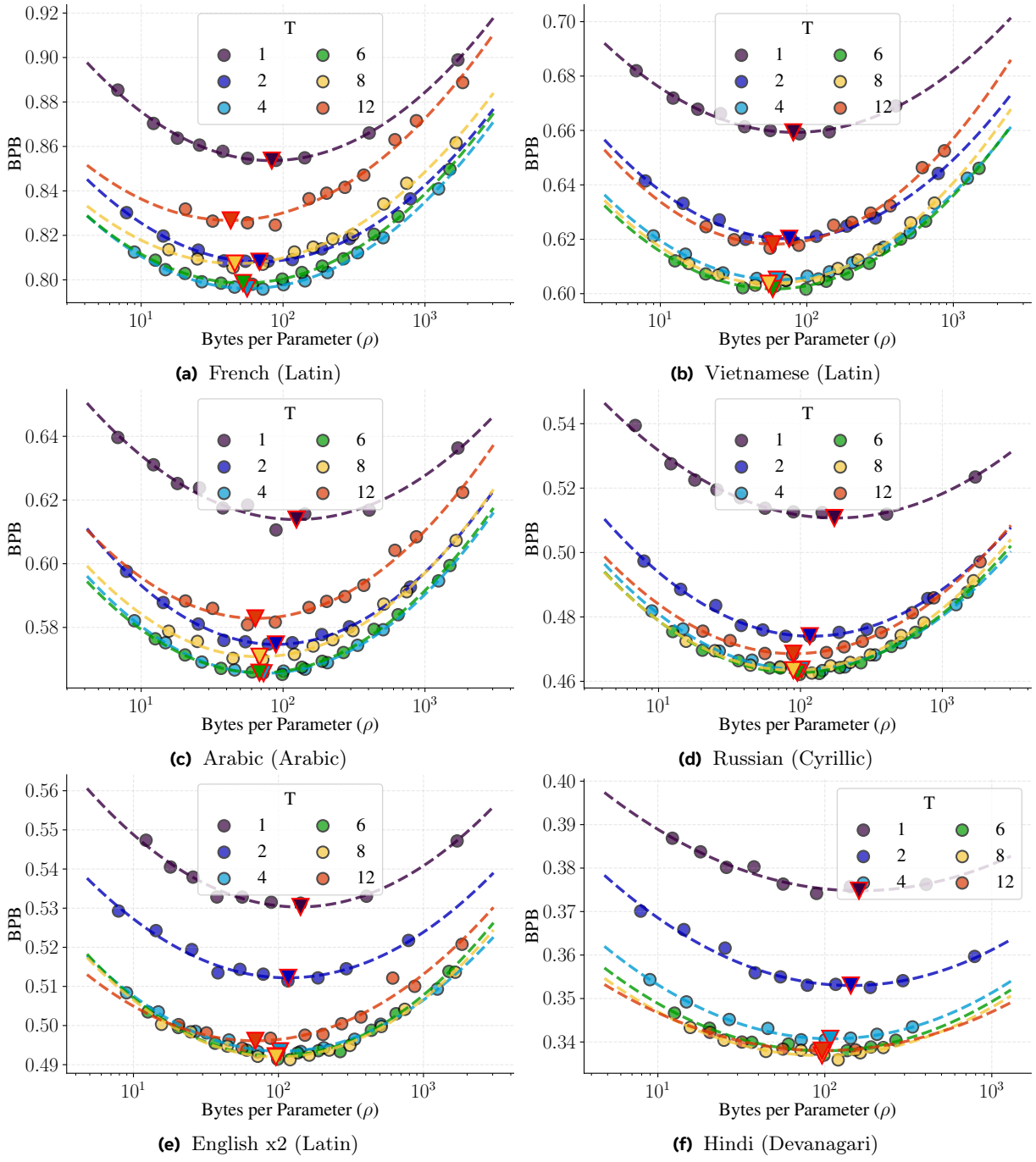

Figure 24 2D IsoFLOP fits across languages ($C = 10^{20}$); all models use latent tokenization to achieve the set compression. Parabolas are fitted for each compression line to interpolate values of the loss.

F.5 Comparison between Character and Byte-level Models

In our analysis of subword tokenized models we focus on character-based instead of byte-based models to examine the properties of low compression. The main difference between these models is that the former has a much larger vocabulary (148,000 vs. 256), while achieving a similar compression rate. In our experiments, we consider character models to coerce on a similar vocabulary size as in BPE and SuperBPE.

We compare the loss of parameter optimal character ($T = 1.01$) and byte models ($T = 1.0$) in Figure 25. Notably, the gap between them is large for a small compute budget due to the relatively high cost of the embedding layer in small models. With the increase of the training budget, the difference narrows. This allows us to assume that character and byte tokenized models will follow similar scaling trends at larger scales. Therefore, in the most of experiments we only consider character-based models.

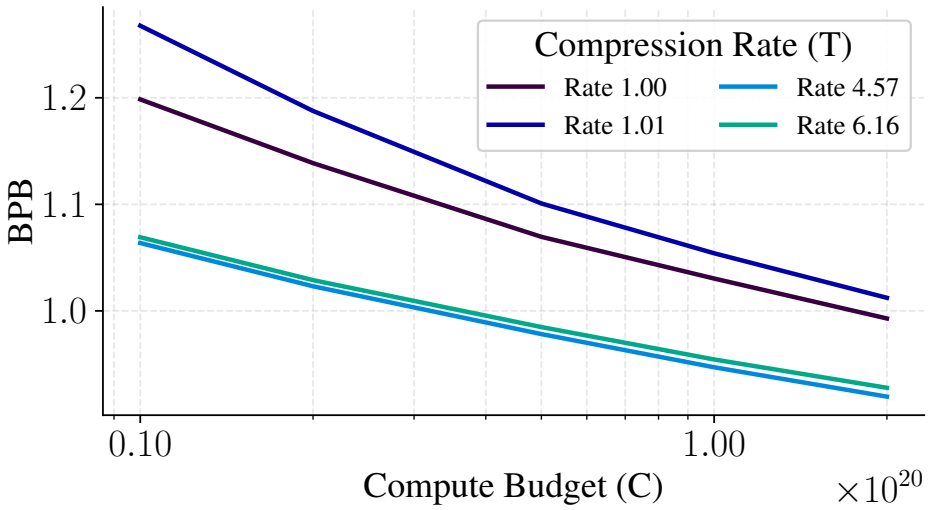

Figure 25 Comparison of optimal test losses for subword tokenized models: byte $T = 1.00$; character $T = 1.01$; BPE $T = 4.57$; SuperBPE $T = 6.16$.

F.6 AI2 Reasoning Challenge Results

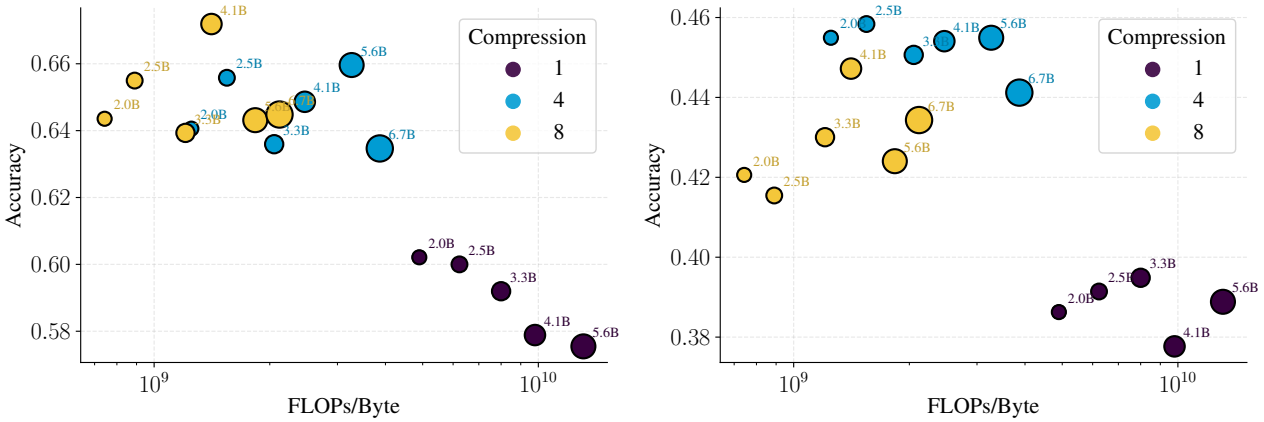

(a) 0-shot Accuracy on ARC-Easy

(b) 0-shot Accuracy on ARC-Challenge

Figure 26 Evaluation of the BLT models trained for $C = 2 \times 10^{21}$ FLOPs on AI2 Reasoning Challange benchmark. The size of each point corresponds to the model parameter count. The results are plotted against inference compute cost per byte, which is dependent on model size N and compression rate T.

Figure 26 presents evaluations on multiple-choice questions from the AI2 Reasoning Challenge (Clark et al., 2018). Interestingly, we observe that for the easier version of the task, models with compression rate 8 and compression rate 4 achieve similar scores. The higher compression (compression rate 8) even obtains the best score for the 4.1B-parameter model, while being cheaper to run than the corresponding compression rate 4 model. On the harder "challenge" split, we observe a different pattern: compression rate 4 achieves higher scores than compression rate 8. We conclude that the choice of optimal compression can be task-dependent. More-compressed, and thus cheaper, tokenization may be adequate for easier tasks, while harder tasks may benefit from the additional inference compute associated with lower compression. We also note the underperformance of byte-level models, which we attribute to insufficient data seen during pre-training.